

CFNS Ad-Hoc meeting on Radiative Corrections Whitepaper

Andrei Afanasev,¹ Jaseer Ahmed,² Igor Akushevich,^{3,4} Jan C. Bernauer,^{5,6} Peter G. Blunden,² Andrea Bressan,^{7,8} Duane Byer,⁹ Ethan Cline,⁵ Markus Diefenthaler,⁴ Jan M. Friedrich,¹⁰ Haiyan Gao,⁹ Alexandr Ilyichev,¹¹ Ulrich D. Jentschura,¹² Vladimir Khachatryan,⁹ Lin Li,¹³ Wally Melnitchouk,¹⁴ Richard Milner,¹⁵ Fred Myhrer,¹³ Chao Peng,¹⁶ Jianwei Qiu,¹⁴ Udit Raha,¹⁷ Axel Schmidt,¹ Vanamali C. Shastry,¹⁸ Hubert Spiesberger,¹⁹ Stan Srednyak,⁹ Steffen Strauch,¹³ Pulak Talukdar,¹⁷ and Weizhi Xiong²⁰

¹*The George Washington University, Washington, DC*

²*University of Manitoba, Winnipeg, MB Canada*

³*Physics Department, Duke University, Durham, NC*

⁴*Jefferson Lab., Newport News, VA*

⁵*Stony Brook University, Stony Brook, NY*

⁶*Riken BNL Research Center, Upton, NY*

⁷*University of Trieste, Dept. of Physics, Trieste, Italy*

⁸*Trieste Section of INFN, Trieste, Italy*

⁹*Duke University, Durham, NC*

¹⁰*Technische Universität München, Physik Dept., Garching, Germany*

¹¹*Institute for Nuclear Problems, Belarusian State University, Minsk, Belarus*

¹²*Missouri University of Science and Technology, Rolla, MO*

¹³*University of South Carolina, Columbia, SC*

¹⁴*Jefferson Lab, Newport News, VA*

¹⁵*Massachusetts Institute of Technology, Cambridge, MA*

¹⁶*Argonne National Laboratory, Lemont, IL*

¹⁷*Indian Institute of Technology Guwahati, Guwahati, Assam, India.*

¹⁸*Regional Institute of Education Mysuru, Mysore, India*

¹⁹*PRISMA+ Cluster of Excellence, Institut für Physik, Johannes Gutenberg Universität Mainz, Mainz, Germany*

²⁰*Syracuse University, Syracuse, NY*

Foreword

Jan C. Bernauer, Jan Friedrich, Haiyan Gao, Richard Milner

Current precision scattering experiments and even more so many experiments planned for the Electron Ion Collider will be limited by systematics. From the theory side, a fundamental source of systematic uncertainty is the correct treatment of radiative effects. To gauge the current state of technique and knowledge, help the cross-pollination between different directions of nuclear physics, and to give input to the yellow report process, the community met in an ad-hoc workshop hosted by the Center for Frontiers in Nuclear Science, Stony Brook University. This whitepaper is a collection of contributions to this workshop.

Radiative effects are classically treated by introducing correction factors to map the measured quantity back to the pure, radiation-effects-free base quantity. For example, a proton form factor experiment actually measures a small energy range of inelastic scattering elements, i.e., those where only a small part of the energy is lost in photons compared to an elastic event. This rate is then mapped back to the elastic rate via correction factors. As can be seen here, this makes the correction not a purely theoretical quantity, as its size depends on the experimental setup, in this case, what energy range is accepted as elastic. To achieve the highest precision, these effective cuts are often better handled not by applying a correction-factor post-hoc, but by integrating the radiative correct cross section into a Monte Carlo simulation.

As such, radiative corrections are really at the interface between experiment and theory, and the problem must be attacked from both directions.

At the same time, experiment design can be affected by considerations of radiative corrections, a detail which is often overlooked. On one hand, choosing suitable detector technologies and experiment kinematics can minimize the uncertainty from radiative corrections, for example due to accurate knowledge of the acceptances relevant for the corrections. On the other hand, added detectors for radiated photons, for example, could reduce the contribution to the measured cross section or allow a calibration of the correction code. Accelerator capabilities like polarization or the change of the particle charge can also be used to measure, or eliminate, radiative corrections.

It is our impression that the field is making good progress on the theory front, with new codes for higher-order corrections becoming available, for example, for electron-proton scattering. The implementation of radiative corrections for jet physics seems also on a good pass, but is maybe somewhat further behind. In general, the path to EIC seems without major obstacles, but we miss a more broad discussion of detector design with regard to radiative corrections. Radiative corrections are often only an afterthought, and we hope that the EIC project will continue to give this important topic enough attention.

The current state of affairs

Jan Friedrich

Practically all scattering reactions of interest in the context of the standard model of particle physics involve the acceleration of electric charge, and modifications due to coupling to the electromagnetic field need to be taken into account in the interpretation of such scattering data.

Already early examinations of quantum electrodynamics have revealed the formal problems dubbed the “infrared catastrophe” [1] for the diverging emission probability for soft photons. The link to a part of the “ultraviolet” divergences was further worked out and led to the successful first-order QED radiative correction scheme as given for electron scattering by Mo and Tsai [2]. For the higher orders, the cancellation of the formally arising divergences was shown, however “in accordance with the usual spirit of perturbation theory,” higher-order finite contributions are ignored “in spite of our complete ignorance of their convergence properties” [3]. The related exponentiation procedure implies the respective uncertainty, unless its validity is proven for finite-energy photons order by order, as is also admitted in modern formulations as [4], that the “next-to-leading terms ... require instead a comparison with the explicit calculation of the cross-section up to the two-loop level”. A complete evaluation of the two-loop level for elastic electron scattering is still not employed beyond the exponentiated form of the one-loop level.

The cross-section for multiple-photon emission, in principle calculable from QED to any order, determines the shape of the radiative tail associated with the elastic process, and especially the region close to the non-radiative elastic kinematics. Experimentally, these effects come together with those of external bremsstrahlung and energy loss of the electrons due to atomic ionisation in the target material. A precise treatment is only possible via Monte Carlo simulations, if credible models for all the contributions are available. For external bremsstrahlung and ionisation energy loss, the model precision is limited by the experimental uncertainties on their empiric parameters [5], and by approximations made for computational efficiency. Regarding the internal photon emission processes, modern generators such

as ESEPP [6] realize only first-order photon emission, based on a photon energy cutoff. This energy cutoff is often argued together with the detector resolution—indeed it does not make much sense to aim at describing features of the peak shape far beyond what is experimentally observable—however the mentioned issues with the exponentiation procedure come on top, and cannot be consistently included in such event generators.

Interesting input can be expected from experiment, if in a well-determined process such as elastic lepton-proton scattering additional photons are observed. The used generators for including radiation effects can then be tested by comparing the observed angular distributions with the shapes expected from QED. Since the effects depend also on the lepton mass, it is foreseen in the Proton Radius Measurement with a 100 GeV muon beam by COMPASS++/AMBER [7] at the CERN SPS M2 beam line, where the bremsstrahlung photons are strongly forward boosted.

Regarding corrections for higher-order contributions due to virtual photons, a similar control is possible by comparing measurements with leptons of positive and negative charge, as continued with the OLYMPUS experiment [8] at DESY.

Key to the implementation of radiative corrections is the consistent split into the theory calculation to determine the “remainder effect” of the regularization procedure for the appearing singularities, and the part which is influenced by the effects of the experimental technique and the cuts applied in the analysis. This becomes a strongly increasing challenge if higher orders and multiple photon emission are to be incorporated. For all the experimental approaches discussed in this white paper, there is a common interest to implement higher-order QED effects in a form such that their analytic parts are well-defined, together with appropriate Monte Carlo methods for the simulation to correct the respective data.

Those efforts are of particular interest in the context of the upcoming Electron-Ion Collider [9] where large effects must be expected due to internal radiation effects accompanying the processes of interest.

Radiative corrections for precision e - p scattering

Jaseer Ahmed, Peter Blunden, Wally Melnitchouk

For many decades the proton's electric ($G_E(Q^2)$) and magnetic ($G_M(Q^2)$) elastic form factors have been measured in unpolarized scattering experiments using the Rosenbluth longitudinal-transverse (LT) separation technique [10–12]. These experiments found that the ratio $\mu_p G_E/G_M$, where μ_p is the proton's magnetic moment, is consistent with 1 over a large range of the four-momentum transfer squared, Q^2 , up to 8.83 GeV². More recently, measurements of the electric to magnetic form factor ratio with significantly reduced uncertainties were performed at Jefferson Lab using the polarization transfer (PT) technique [13–17]. These experiments found a linear fall-off of the ratio $\mu_p G_E/G_M$ from 1 with increasing Q^2 in the range up to 8.5 GeV².

Analysis of the LT-separated electron scattering data has traditionally been performed within the one-photon exchange (OPE) approximation. The electric to magnetic form factor ratio discrepancy motivated studies of hadron structure-dependent two-photon exchange (TPE) radiative corrections, and it was generally believed that the problem would be resolved with the inclusion of these effects [18, 19].

The use of hadronic degrees of freedom can be considered as a reasonable approximation for low to moderate values of $Q^2 \lesssim 5$ GeV², where hadrons are expected to retain their identity. On-shell form factors are used explicitly to calculate the imaginary part of the TPE amplitude from unitarity, with the real part then obtained from a dispersion integral. In our work [20] we follow the dispersive approach for resonant intermediate states developed in Ref. [21]. We account for all four and three-star spin-1/2[±] and spin-3/2[±] resonances with mass below 1.8 GeV from the Particle Data Group [22], which include the six isospin-1/2 states $N(1440)$, $N(1520)$, $N(1535)$, $N(1650)$, $N(1710)$ and $N(1720)$, and the three isospin-3/2 states $\Delta(1232)$, $\Delta(1620)$ and $\Delta(1700)$. We allow for a Breit-Wigner shape with a nonzero width for each individual resonance, with either a fixed width or a dynamical width that depends on the final state hadron mass. In our numerical calculations, for the resonance electrocouplings at the hadronic vertices we use the most recent helicity amplitudes extracted from the analysis of CLAS electroproduction data [23, 24], except for the $\Delta(1232)$ resonance, for which we use the fit by Aznauryan and Burkert [21, 25]. For the elastic intermediate state contribution, we use the parametrizations from Kelly [26], which have poles only in the timelike region of Q^2 .

The TPE correction δ is defined via

$$\frac{d\sigma}{d\Omega} = \left(\frac{d\sigma}{d\Omega} \right)_{\text{Born}} (1 + \delta). \quad (1)$$

The combined effect on δ from the nucleon plus all the spin-parity 1/2[±] and 3/2[±] resonances is illustrated in

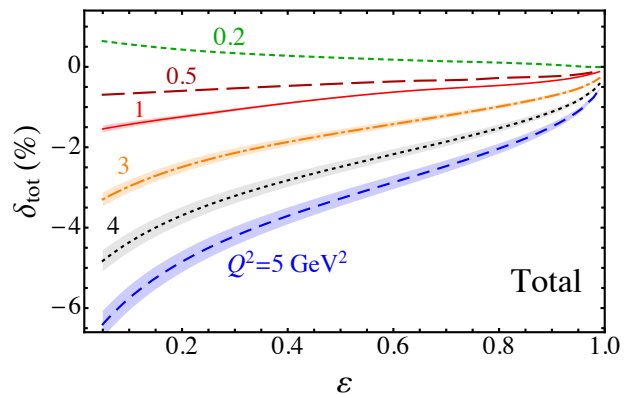


FIG. 1. The total TPE correction δ (in %) versus ϵ for nucleon plus all spin-parity 1/2[±] and 3/2[±] resonances at $Q^2 = 0.2$ GeV² (green dashed line), 0.5 GeV² (dark red long-dashed), 1 GeV² (red solid), 3 GeV² (orange dot-dashed), 4 GeV² (black dotted), and 5 GeV² (blue dashed). The shaded bands correspond to the uncertainty propagated from the input electrocouplings.

Fig. 1 as a function of virtual photon polarization, ϵ , for a range of fixed Q^2 values between 0.2 and 5 GeV². At low $Q^2 \lesssim 3$ GeV², the net excited state resonance contribution is found to be small, and the total correction is dominated by the nucleon elastic intermediate state. The net effect of the higher mass resonances is to increase the magnitude of the TPE correction at $Q^2 \gtrsim 3$ GeV², due primarily to the growth of the (negative) odd-parity $N(1520)$ and $N(1535)$ resonances, which overcompensates the (positive) contributions from the $\Delta(1232)$. At the highest $Q^2 = 5$ GeV² value, the total TPE correction δ_{tot} reaches $\approx 6\%$ - 7% at low ϵ .

An estimate of the theoretical uncertainties on the TPE contributions can be made by propagating the uncertainties on the fitted values of the transition electrocouplings [24], which are dominated by the $\Delta(1232)$ and $N(1520)$ intermediate states. At low Q^2 , $Q^2 \lesssim 0.5$ GeV², the uncertainties are insignificant, but become more visible at higher Q^2 values, as illustrated by the shaded bands in Fig. 1, for $Q^2 = 1$ - 5 GeV².

Perhaps the most direct consequence of TPE is the deviation from unity of the ratio of e^+p to e^-p elastic scattering cross sections, which behaves like $R_{2\gamma} = \sigma(e^+p)/\sigma(e^-p) \approx 1 - 2\delta$, and is a direct measure of the TPE correction δ . Recent experiments at Jefferson Lab [27], Novosibirsk [28] and DESY [29] have attempted more precise determinations of $R_{2\gamma}$ over a larger range of Q^2 and ϵ values than previously available.

The OLYMPUS experiment at DESY [29] measured the ratio $R_{2\gamma}$ over a range of ϵ from ≈ 0.46 to 0.9 at an electron energy $E \approx 2$ GeV, with Q^2 ranging up to ≈ 2 GeV². The results, illustrated in Fig. 2, indicate an

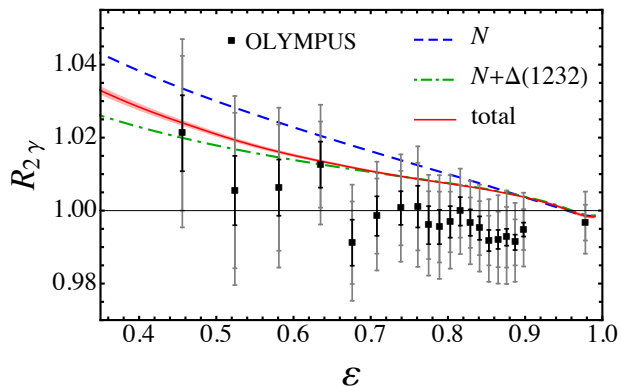


FIG. 2. Ratio $R_{2\gamma}$ versus ϵ from the Ref. [29], compared with the nucleon only (blue dashed line), sum of nucleon and $\Delta(1232)$ (green dot-dashed line), and sum of all intermediate state contributions (red solid line and band). The experimental statistical and systematic uncertainties are indicated by the (black) inner and (gray) outer error bars, respectively.

enhancement of the ratio at $\epsilon \lesssim 0.6$ and a dip below unity at $\epsilon \gtrsim 0.7$, although still compatible with no deviation from 1 within the combined statistical and systematic uncertainties. The suppression of the ratio at large ϵ is in tension with other measurements, but the effect is consistent within the errors [21]. Inclusion of the $\Delta(1232)$ intermediate state reduces the effect of the nucleon elastic contribution away from the forward scattering region, but the effect of the higher mass resonances is very small for all ϵ shown. The overall agreement between the TPE calculation and the OLYMPUS data is reasonable within the experimental uncertainties, although there is no indication in our model for a decrease of the ratio below unity at large ϵ .

The most widely discussed consequence of TPE over the last two decades is the ratio $\mu_p G_E/G_M$ extracted using the LT separation method [18]. The TPE correction induces an additional shift in the ϵ dependence of the reduced cross section, which affects the extraction of both G_E and G_M . To extract G_E and G_M it is appropriate to correct the data for TPE contributions at the same level as other radiative corrections in order to obtain the genuine Born contribution.

In Fig. 3 we show the G_E/G_M ratio extracted from our analysis for the SLAC [10, 11] and Jefferson Lab Super-Rosenbluth [12] experiments up to $Q^2 = 5 \text{ GeV}^2$. To avoid clutter, the PT data from Refs. [13–17] are shown as a band, which is a nonlinear fit at the 99% confidence limit. The original analysis, shown in Fig. 3(a), is consistent with $\mu_p G_E/G_M \approx 1$, while a progressively larger effect of TPE with increasing Q^2 for all LT data sets is seen in Fig. 3(b), with a commensurate increase in the uncertainty of G_E . In particular, the LT data of Andivahis *et al.* [11] are striking in their consistency with the

PT band, with a near linear falloff of G_E/G_M with Q^2 . These results provide compelling evidence that there is no inconsistency between the LT and PT data once improvements in the RCs and TPE effects are made.

Future precision measurements at higher Q^2 values and backward angles (small ϵ), where TPE effects are expected to be most significant, would be helpful for better constraining the TPE calculations. This would provide a more complete understanding of the relevance of TPE in the resolution of the proton's G_E/G_M form factor ratio puzzle, and better elucidate the role of multi-photon effects in electron scattering in general.

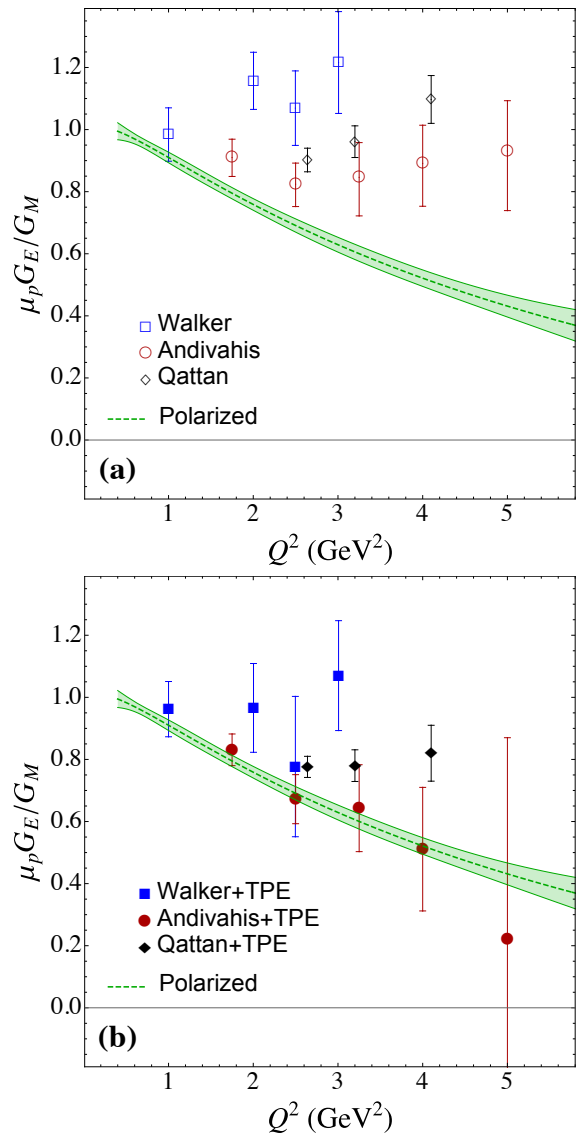


FIG. 3. (a) Ratio $\mu_p G_E/G_M$, versus Q^2 , extracted using LT separation data [10–12]. A nonlinear fit to the combined PT results [13–17] at the 99% confidence limit is shown by the green band. (b) The ratio $\mu_p G_E/G_M$ extracted from a reanalysis of the LT data using improved standard RCs from Ref. [30], together with the TPE effects from our work [20].

Radiative corrections and two-photon exchange for MUSE and JLAB

Andrei Afanasev, Alexandr Il'yichev

Development of consistent approaches to QED corrections in lepton-nucleon scattering is crucial for precision analysis of nucleon's structure. While at JLab energies ultra-relativistic approximation is well justified for GeV electrons (except for very forward scattering angles), for MUSE muons with momenta in 100s MeV/c, the lepton mass effects have to be treated without assuming the small-mass limit. MUSE experiment aims to compare electron-proton and muon-proton cross sections with percent accuracy and probe two-photon effects via measurements of a charge asymmetry in the scattering of leptons vs anti-leptons. In addition to purely kinematic mass effects, interaction dynamics for muons contains new contributions, as we discuss below.

Leading-order QED corrections to electron or muon scattering on a nucleon responsible for charge asymmetries are represented by the diagrams in Fig. 4.

We have upgraded a Monte-Carlo generator ELRADGEN [31] to include lepton masses without using an ultra-relativistic approximation. QED corrections due to model-independent emission from leptons is shown in Fig. 5, calculated using ELRADGEN in MUSE kinematics. Considering only soft-photon corrections, the contributions of the diagrams Fig. 4 to scattering observables were calculated analytically in Ref.[32] without using a small-mass approximation for the scattering leptons, and charge asymmetries were predicted for a wide

range of kinematics, including MUSE.

Among the dynamic effects different for muons and electrons beyond the leading order in QED, we should mention enhancement of helicity-flip amplitude for massive muons that makes a noticeable contribution to the two-photon correction [33] via t -channel σ -meson exchange; and a single-spin beam asymmetry for polarized muons (coming from weak decay of pions) that generates an azimuthal dependence of scattering cross section [34]. Two-photon corrections to muon-proton scattering were also considered in Ref.[35].

The next step was made recently [36] with inclusion of the emission of *hard* photons to describe charge asymmetries in scattering of electrons and muons on a proton. While hard-photon emission may be constrained by kinematic cuts in experimental analysis, its inclusion is necessary for complete analysis, especially the events located further away from the elastic peak on a radiative tail.

In summary, the main contributions to QED corrections for lepton-proton scattering were calculated and implemented in Monte-Carlo code ELRADGEN. The code can be used for MUSE kinematics, where ultra-relativistic approximation is no longer applicable for the muons, as well as at JLab and other facilities, where lepton mass effects play a role at very forward scattering angles (e.g., in PRAD experiment at JLab). Two-photon effects are included in a soft-photon-exchange approximation, while keeping options to include additional model-dependent two-photon contributions. The code can be downloaded from <http://www.jlab.org/RC>.

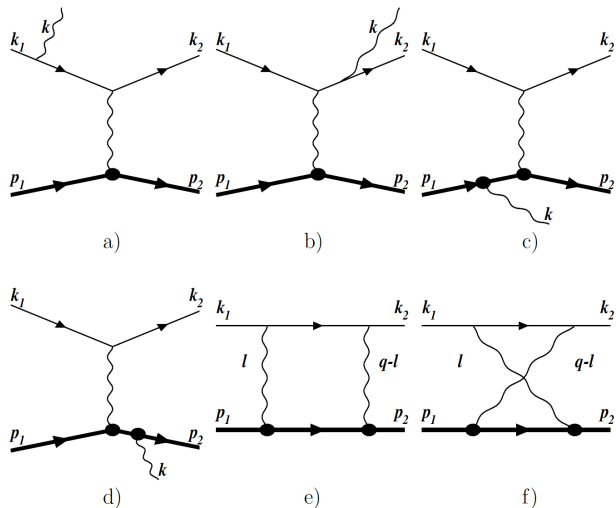


FIG. 4. Feynman diagrams for leading-order QED corrections responsible for charge asymmetries in lepton-proton scattering. The charge asymmetry is due to interference between one-photon exchange contribution and diagrams (c,d), as well as interference between photon emission from the lepton (a,b) and the proton.

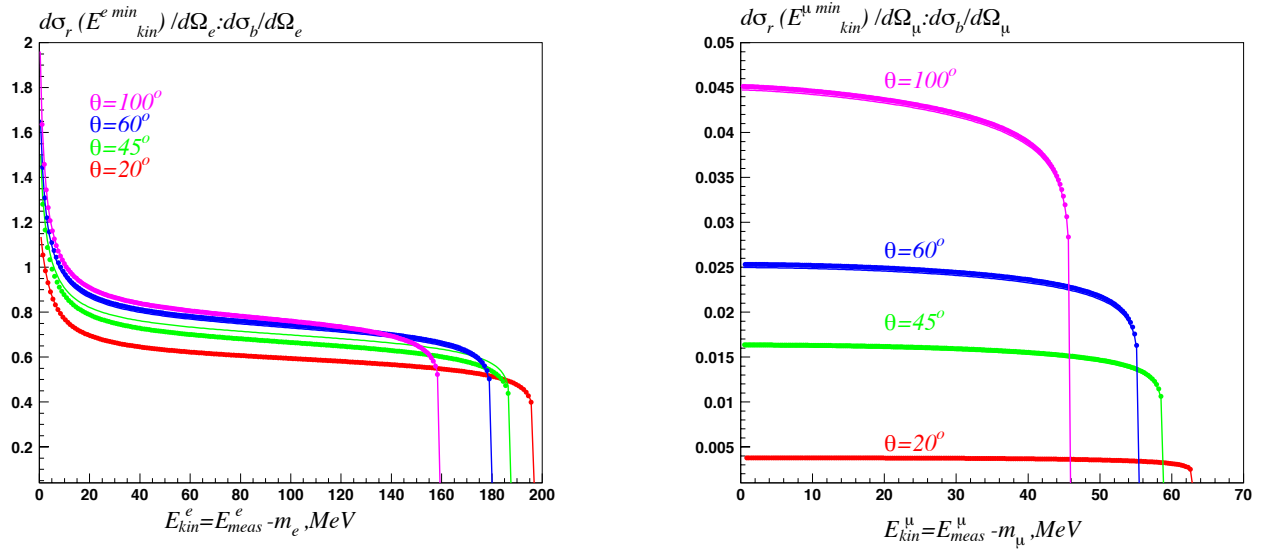


FIG. 5. QED correction to the cross section of electron-proton scattering (left plot) and muon-proton scattering (right plot) in MUSE kinematics as a function of final lepton energy plotted for different scattering angles. The correction for electrons is larger and it is strongly peaked for nearly stopped final electrons, which makes it sensitive to energy cuts. The correction to muons is smaller, at one per cent level, and does not show drastic variation with final-muon energy.

Radiative corrections for the MUSE experiment

Lin Li, Steffen Strauch

MUON SCATTERING EXPERIMENT (MUSE)

The MUon Scattering Experiment (MUSE) at the Paul Scherrer Institute (PSI) [37] has been developed to measure elastic electron-proton and muon-proton scattering cross-sections of positively and negatively charged leptons and beam momenta between 115 MeV/c and 210 MeV/c over a wide angular range. MUSE covers a four-momentum-transfer range from $Q^2 = 0.002$ to 0.08 GeV^2 . Each of the four sets of data will allow the extraction of the proton charge radius. In combination, the data test possible differences between the electron and muon interactions and, additionally, two-photon exchange effects.

Figure 6 shows a sketch of the experimental setup of MUSE at the secondary π M1 beamline at PSI. The particle beam contains a mix of electrons, muons, and pions. These particles go through the Beam Hodoscope (BH) detector for timing and particle identification. The BH also measures the beam fluxes. Three Gas Electron Multiplier (GEM) chambers determine the incident particle track. A veto detector suppresses triggers from off-axis particles. Particles that scatter from the Liquid Hydrogen target are detected by two symmetric spectrometers, each with two Straw-Tube Tracker (STT) chambers and

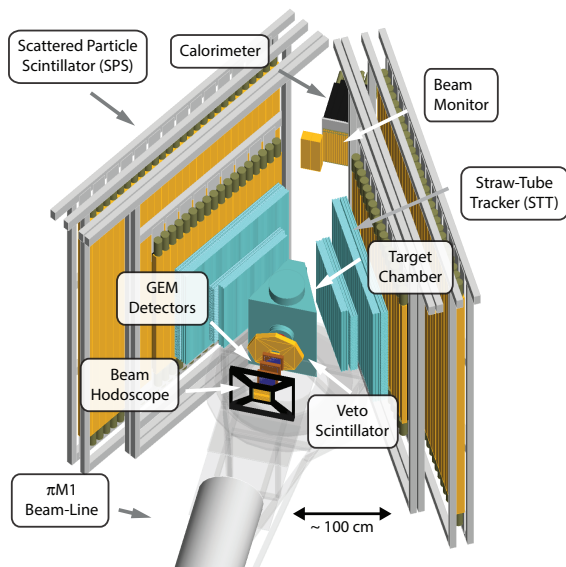


FIG. 6. Sketch of the MUSE experimental setup at the π M1 beamline at PSI as implemented in the MUSE Geant4 simulation. The target chamber contains liquid-hydrogen, empty, and solid targets.

two planes of fast Scattered Particle Scintillators (SPS). The two SPS planes (front-wall and rear-wall) provide the event trigger which requires an above-threshold ($E_{th} = 2 \text{ MeV}$) hit in each scintillator wall. The threshold for detecting electrons is around $10 \text{ MeV}/c$. The unscattered particles go through the Beam Monitor (BM). The time-of-flight (TOF) from BH to SPS determines the reaction type (muon scattering vs. muon decay in flight). TOF from BH to BM identifies backgrounds and determines μ and π beam momenta. The BM can also be used to suppress Møller events. Downstream of BM is a calorimeter which is used to detect photons radiated from particles.

RADIATIVE CORRECTIONS FOR MUSE

For each bin of the scattering angle, MUSE will measure the integrated electron-proton and muon-proton yields that includes all events in the spectrometer acceptance and momenta above the detection threshold of $p'_{\min} \approx 10 \text{ MeV}/c$. The magnitude of the momenta of the final-state leptons remain otherwise unmeasured. The Born cross-section, that contains information about the electromagnetic form factors, is obtained from the experimental cross-section, $(d\sigma/d\Omega)$, with a correction, $1 + \delta$, for higher-order processes, including the first-order bremsstrahlung process, the vacuum polarization correction, the vertex corrections, and the two-photon-exchange corrections, e.g., [38],

$$\left(\frac{d\sigma}{d\Omega}\right) = \left(\frac{d\sigma}{d\Omega}\right)_{\text{Born}} (1 + \delta). \quad (2)$$

Besides the internal processes where a photon is emitted during the lepton-proton scattering, the external processes accompanying the passage of incident and outgoing particles through the upstream detector and target materials have to be considered. To study the full effect, a Monte Carlo simulation with an event generator is being implemented for MUSE. An event generator for MUSE must fulfill several requirements. First, the event generator should include the emission of a hard radiated photon, which is beyond the soft-photon approximation. The hard photon needs to be propagated in the full Monte Carlo simulation. Second, the event generator needs to include the mass of the leptons, avoiding the $Q^2 \gg m^2$ approximation in the calculation. The Elastic Scattering of Electrons and Positrons on Protons (ESEPP) event generator [6] takes into account the first-order radiative corrections of elastic scattering of charged leptons (e^\pm and μ^\pm) on protons and fulfills these requirements. We have used ESEPP for our preliminary studies.

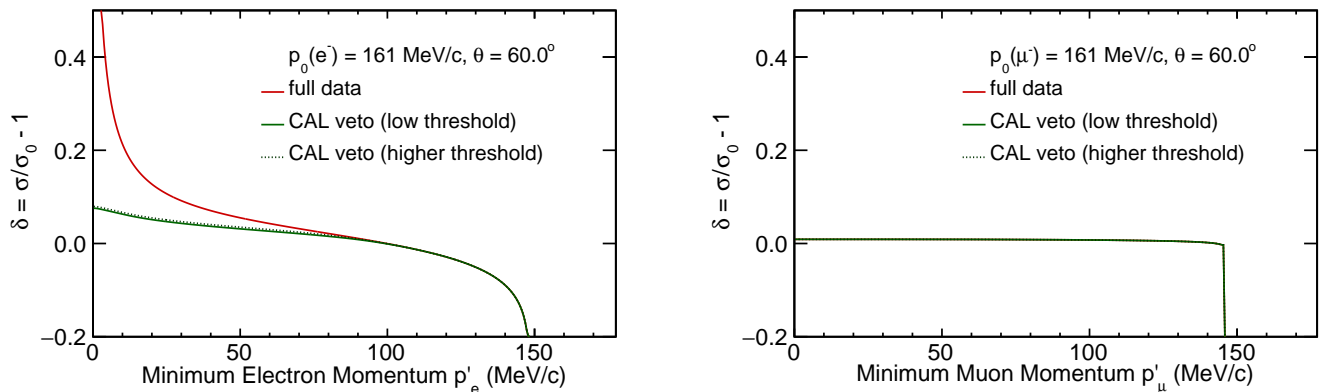


FIG. 7. Preliminary radiative corrections for ep (left) and μp (right) scattering in typical MUSE kinematics. The red curve shows the full result without a photon veto. The green curves are after suppression of initial-state radiation and include a veto on events with a hit in the calorimeter at different thresholds.

Other generators that are viable for MUSE include those of Refs. [6, 39–41].

The internal radiative correction δ depends on the kinematics of the reaction and detector properties. Uncertainties in the knowledge of these parameters propagate into uncertainties in the corrections. Using ESEPP, we studied the dependence of δ on the beam momentum, scattering angle, and the minimum lepton momentum p'_{\min} , and found the largest sensitivity due to p'_{\min} . Preliminary results for δ are shown in Fig. 7 as a function of p'_{\min} for electron (left panel) and muon (right panel) beams of a momentum of 161 MeV/c and for a mid-range scattering angle of 60° . The red curves show the results for all scattering events, regardless of the emission of photons. It shows a strong dependence on p'_{\min} with a steep slope ($> 1\%$ change per 1 MeV/c) close to the SPS detection threshold of 10 MeV/c. If uncontrolled, the uncertainty in p'_{\min} would generate a considerable uncertainty in δ . The simulations reveal that the increase in δ with a decrease in p'_{\min} is linked to the increase of the ep cross-section with reduced beam momentum after the emission of high-energy initial-state radiation. The initial-state radiation is strongly forward peaked, and the MUSE calorimeter in the beamline downstream of the target is capable of detecting these Bremsstrahl photons. The green curves in Fig. 7 show the results for δ after vetoing those events with a detected photon. The difference between the solid and dashed green curves is in different photon-detection thresholds in the calorimeter. The radiative corrections are smaller after the suppres-

sion of initial-state radiation, and the dependence on p'_{\min} is reduced. Radiative corrections for muons are much smaller than for electrons and nearly independent on p'_{\min} , as shown in the right panel of Fig. 7. Because there are not many photons emitting from muons to the forward direction, the calorimeter cut does not affect the data.

Considering all the kinematic settings, the preliminary estimates of the uncertainties in the radiative corrections are 0.4% to 0.8% for electrons and smaller than 0.06% for muons.

SUMMARY AND OUTLOOK

MUSE is a high-precision experiment to measure the proton charge radius, study possible 2γ mechanisms, and have a direct μ/e comparison of the elastic cross-sections. Without a magnetic spectrometer, MUSE does not measure the final-state lepton momentum precisely. A dedicated downstream photon detector helps to suppress initial-state radiation effects. Preliminary ESEPP simulations show uncertainties in the radiative corrections for electron scattering to be lower than 1%. Ongoing work includes implementing the event generator in a full MUSE simulation. After data taking, the analysis allows for moderate changes in the SPS lepton-momentum detection threshold. Those changes will affect radiative corrections. Consistent cross-sections extractions for various values of p'_{\min} test the validity of the corrections.

Modeling Radiative Processes for the OLYMPUS Experiment

Axel Schmidt

The OLYMPUS Experiment [8] was one of three recent experiments to quantify the effects of hard two-photon exchange (TPE) in elastic electron-proton scattering [8, 42, 43]. OLYMPUS measured the ratio of positron-proton to electron-proton elastic scattering cross sections, a ratio where deviations from unity are evidence of TPE. The goal of these experiments was to test whether the effects of hard TPE are sufficient to explain the discrepancy between polarized and unpolarized measurements of the proton form factor ratio $\mu G_E/G_M$. Hard TPE is a radiative correction that has been typically assumed to be negligible, and one reason is that it cannot be calculated in a model independent way. By contrast, soft TPE—calculated in the limit in which one exchanged photon carries negligible momentum—is included in standard radiative correction formulae [2, 38], though with slight differences in definition.

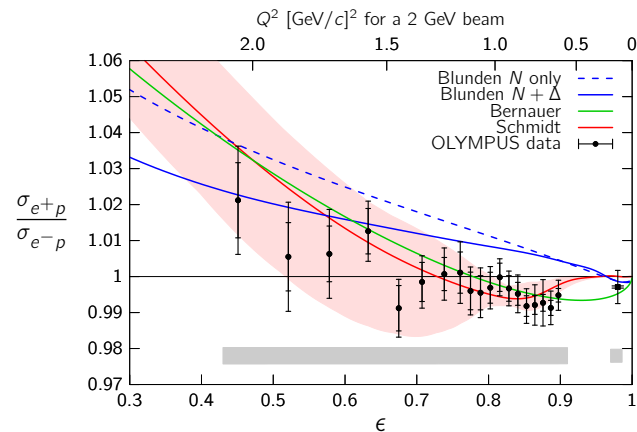


FIG. 8. The OLYMPUS results [8] compared with the theoretical predictions of Blunden and Melnitchouk [44], and the phenomenological predictions of Bernauer et al. [45] and Schmidt [46]. Though the data don’t show large deviations from unity, the results are consistent with the size of the proton form factor discrepancy in the kinematics probed.

The results of the OLYMPUS Experiment are shown in Fig. 8, and compared to several predictions. The results show evidence of a small hard TPE effect. The data fall slightly below the dispersive hadronic calculations of Blunden and Melnitchouk [44], and agree better with phenomenological predictions [45, 46] made from the size of the proton form factor discrepancy. This suggests that even though the measured hard TPE effect is small, it is fully consistent with the hypothesis that it is the cause of the form factor discrepancy. A more definitive measurement is needed at higher Q^2 / lower ϵ . This would be particularly useful for testing partonic calculations of hard TPE (e.g., Refs. [47, 48]). The findings of these experiments and a summary of the current status

of two-photon exchange can be found in Ref. [49].

Accurately modeling radiative effects was important in OLYMPUS because isolating the effects of hard TPE meant also accounting for other radiative processes that introduce an asymmetry between positron-proton and electron-proton cross sections. In addition to soft TPE, the effects of interference between lepton-leg bremsstrahlung with proton-leg bremsstrahlung are also lepton-charge odd. These effects are treated in the standard radiative corrections formulae, but treating radiative corrections as a simple multiplicative factor was inappropriate for OLYMPUS for two reasons.

1. OLYMPUS was a coincidence measurement, and elastic event selection was made on non-trivial exclusivity cuts.
2. OLYMPUS did not have excellent momentum resolution, meaning that the elastic event sample had an unavoidable contribution from events with a hard radiated photon.

Given this situation, we chose to model radiative effects using simulation and to write a custom event generator, described in Chap 5 of Ref. [50]. We then used the generator to integrate the radiative elastic cross section over the phase space defined by the elastic event selection criteria.

One major design question we had to confront was whether or not to use exponentiation to attempt to treat radiation beyond the α^3 order. Exponentiation can be used to treat radiation to all orders in the soft limit [3]. However, the limits of the OLYMPUS detector resolution required us to model radiation in the deep tail. We decided to try both exponentiated and non-exponentiated approaches and to compare results.

NON-EXPONENTIATED APPROACH

In the non-exponentiated approach, we set an arbitrary cut-off energy (with a value much smaller than the detector resolution, typically about 1 MeV) below which the event was considered to be “near-elastic” and above which the event was considered part of the “hard tail.” In the near-elastic regime, a standard multiplicative correction was used, i.e.,

$$\frac{d\sigma}{d\Omega} = \frac{d\sigma}{d\Omega}_{\text{Born}} (1 + \delta(\Delta E_{\text{cut-off}})).$$

In the hard tail, the cross section was assumed to be the tree-level bremsstrahlung cross section, taking care to include all of the interferences terms of all of the diagrams. The non-exponentiated approach essentially used

the same cross section model as employed in the ESEPP Generator developed for the Novosibirsk two-photon experiment [6].

EXPONENTIATED APPROACH

The exponentiated approach was developed from an earlier generator produced by the Mainz A1 collaboration (and described in Ref. [40]). While the phase space for electron-proton scattering with multiple undetected hard bremsstrahlung photons is six-dimensional (three degrees of freedom for the electron momentum, three degrees of freedom for the proton momentum), we first made the simplifying assumption that the kinematics were well-described by the five-dimensional phase space in which only one radiated photon is hard. Next, we assumed that radiated cross section could take an exponential form, i.e.,

$$d^5\sigma = \frac{d\sigma}{d\Omega_{\text{Born}}} e^\delta (\partial_{\vec{\gamma}}\delta), \quad (3)$$

where $(\partial_{\vec{\gamma}}\delta)$ is the differential change cross section with respect to the momentum of the hard photon. We assumed that this could be approximated by the ratio of the tree-level bremsstrahlung cross section to the elastic ep cross section, and that the e^δ correction factor could be taken from a standard radiative correction. The final model cross section was given by:

$$d^5\sigma = e^\delta \times d^5\sigma_{\text{brems.}} \quad (4)$$

RESULTS

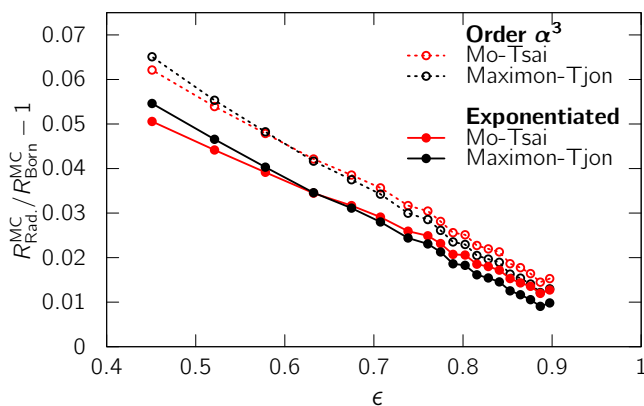


FIG. 9. The charge-odd radiative corrections in OLYMPUS were several times bigger than the hard TPE effect.

The approximate size of the charge-odd radiative correction in OLYMPUS is shown in Fig. 9 for both the exponentiated and non-exponentiated (Order α^3) approaches, for the different definitions of soft TPE employed by Mo and Tsai [2] and Maximon and Tjon [38]. In both approaches, the correction grows as ϵ decreases, reaching 5–7%, i.e., the measured hard TPE effect sat on top of a baseline ratio that was 5–7% higher than unity due to soft TPE and bremsstrahlung interference. These radiative effects were several times bigger than the effect of hard TPE itself. The exponentiated approach predicted a smaller correction than the non-exponentiated approach; however, the difference was relatively small compared to the magnitude of the correction.

The OLYMPUS results were published relative to all four corrections, to allow the reader to judge based on the correction they deem most appropriate [8].

FUTURE PLANS

There are two obvious things that could be added to the OLYMPUS generator. First is the inclusion of models of hard TPE, in order to see how these effects would propagate through the entire simulation. Second is the inclusion of off-shell currents when calculating the matrix elements for bremsstrahlung emitted from the proton. So far, the OLYMPUS generator assumes on-shell currents even for these off-shell vertices. This would probably have a minute effect on the results, but is an easy improvement to make.

OLYMPUS has recently submitted for publication the results of the lepton-charge average cross section (i.e. $\frac{1}{2}[e^+p + e^-p]$), a combination in which charge-odd effects like TPE cancel at lowest order [51]. This observable can give direct information about the proton's form factors, while being much more robust to any bias from TPE.

A paper describing the OLYMPUS generator in detail is in preparation and will hopefully be useful to future high-precision elastic scattering experiments, such as MUSE at PSI [37], the prospective TPEX project at DESY, or future experiments suggested by the Jefferson Lab positron working group [52].

Radiative correction studies for the PRad and proposed PRad-II, DRad and SoLID experiments at Jefferson Laboratory

Vladimir Khachatryan, Duane Byer, Haiyan Gao, Chao Peng, Weizhi Xiong

RADIATIVE CORRECTION STUDIES FOR THE PRAD EXPERIMENT

In order to reach a high precision in proton (deuteron) radius measurements from electron scattering, in addition to a tight control of various experimental systematic uncertainties, a careful calculation of radiative corrections (RC) is necessary. A recent measurement of the charge radius of the proton was performed by the PRad experiment, which measured the unpolarized elastic $e + p$ scattering cross section and the proton electric form factor in an unprecedentedly low momentum transfer squared region: $Q^2 = 2.1 \cdot 10^{-4} - 6 \cdot 10^{-2} \text{ (GeV/c)}^2$, equivalent to the scattering angle in the laboratory frame, $0.8^\circ \leq \theta \leq 7^\circ$. During the PRad experiment the luminosity was monitored by simultaneously measuring the Møller scattering process, and the absolute $e - p$ elastic scattering cross section was normalized to that of the Møller to cancel out the luminosity. Therefore, the RC effects have been studied for both scattering processes. The extracted value of the proton radius turned out to be $r_p = 0.831 \pm 0.007_{\text{stat}} \pm 0.012_{\text{sys}} \text{ fm}$ [53, 54], with the RC being one of the largest systematic uncertainty sources.

Ref. [55] shows a complete set of analytical expressions for calculating the one-loop RC diagrams to $e - p$ and Møller scatterings, obtained within a covariant formalism and beyond the ultrarelativistic approximation, where the infrared divergence is extracted and canceled using the Bardin-Shumeiko approach [56]. A related event generator has been built, which included RC contributions to the Born cross sections of these scattering processes [57]. PRad has estimated the uncertainty on the measured proton radius based upon the first order RC results from [55], and also using the method of [58] for estimation of the contribution coming from higher order RC. The estimated systematic uncertainties for both $e - p$ and Møller scatterings are correlated and Q^2 -dependent. The Q^2 -dependence is much larger for the Møller RC, and it affects the cross section results through the use of the bin-by-bin method [54]. If one transforms the cross section uncertainties into the uncertainties of r_p , then for $e - p$ we have $\sim 0.0020 \text{ fm}$, and for the Møller we have $\sim 0.0065 \text{ fm}$, such that the total systematic uncertainty due to the higher order RC is equal to $\delta r_p = 0.0069 \text{ fm}$.

Given that the Q^2 -dependent systematic uncertainty is much larger for the Møller scattering, PRad has performed an independent estimate for the second order RC effect on r_p . This estimate follows the method shown in [59] (developed for the MOLLER experiment at JLab), where the authors have calculated two-loop electroweak corrections to the parity violating asymme-

try to the Møller scattering in the MOLLER kinematic range. Based on their mathematical framework, we were able to estimate the contribution from the next-to-next leading order (NNLO) diagrams to the Born cross section in the PRad kinematic range (however, considering only restricted number of diagrams). The estimated Q^2 -dependent systematic uncertainties are smaller than those estimated in the first approach, for any reasonable photon energy cut for the PRad experiment. We obtained a few values of δr_p , with the largest one being 0.0047 fm , which is well within the first estimate. Thus, we still use the uncertainty of $\delta r_p = 0.0069 \text{ fm}$ due to RC effects as a conservative estimate on r_p for PRad.

PLANNED RADIATIVE CORRECTION STUDIES FOR THE PROPOSED PRAD-II EXPERIMENT

The proposed PRad-II experiment at JLab [60] – an enhanced and improved version of the PRad experiment – has a factor of 3.8 smaller estimated total uncertainty on r_p than that of PRad. The PRad-II experiment will have projected total uncertainty of 0.43%, by which one could address the possible systematic differences between $e - p$ and μH experiments, as well as between the PRad and other recent $e - p$ scattering experiments. The improvements that PRad-II will achieve in reducing the key systematic uncertainties as compared to PRad, includes in particular the installation of planes of high spatial-resolution tracking detector based on the μRWELL , by which the detector efficiency determination will be much more precise. In the PRad experiment, one plane of GEM detectors was used for tracking. As it is shown in the PRad-II proposal, the Q^2 -dependent systematic uncertainties from the Møller scattering can be suppressed by using the integrated Møller method for all angular bins [54], which will turn all systematic uncertainties from the Møller into normalization uncertainties for the cross sections. This method is fully applicable for PRad-II due to presence of the two planes of tracking detectors, releasing us from the need of using the bin-by-bin method. Based on the studies for PRad-II, the RC uncertainty of r_p coming from the integrated Møller method will be significantly reduced by a factor of ~ 4 .

However, it would be very relevant to calculate the higher order RC contribution from the theory side as well. Along with other improvements in reducing the r_p systematic uncertainties (see [60]), one more key factor is our planned new RC calculations to further improve the precision in determination of the proton radius. In this connection we should note that one of priority goals of PRad-II is to calculate exactly the next-to-

next-leading (NNLO) RC diagrams in unpolarized elastic $e - p$ and Møller scatterings beyond ultrarelativistic limit for the PRad-II kinematics: namely, in the region of $Q^2 \sim 10^{-5} - 6 \cdot 10^{-2} (\text{GeV}/c)^2$, corresponding to the scattering angle in the laboratory frame, $0.5^\circ \leq \theta \leq 7^\circ$. Currently our theory collaborators are developing a new method [61], where the calculated results, namely amplitudes or cross sections, can be represented as power series that are convergent on the chain of integration of the corresponding integrals. With this method one may be able to calculate all necessary NNLO diagrams. The current PRad event generator [57], which is made based upon the NLO results from [55], will be modified and developed accordingly, along with upcoming new results.

PLANNED RADIATIVE CORRECTION STUDIES FOR THE PROPOSED DRAD EXPERIMENT

The PRad collaboration has also proposed the DRad experiment [62] for the deuteron charge radius measurement at JLab, with recently estimated total uncertainty on extracted r_d to be 0.22%. In general, this experiment aims to accomplish a new high precision unpolarized elastic $e - d$ scattering cross section measurement in the low- Q^2 region of $2 \cdot 10^{-4} - 5 \cdot 10^{-2} (\text{GeV}/c)^2$, using the PRad experimental setup with some modifications. All the Møller RC studies, which will be done for PRad-II, will be likewise applicable for DRad. However, for the studies of radiative effects in $e - d$ scattering, first we need to revise the papers [63, 64] and fulfill complete calculations of the NLO RC diagrams in unpolarized elastic $e - d$ scattering beyond ultrarelativistic limit for the DRad kinematics, by using the most recent charge, magnetic and quadrupole form factors of the deuteron. Accordingly, a new $e - d$ event generator will be created, which will replace the current existing one that is based on the soft photon approximation [65].

ONGOING RADIATIVE CORRECTION STUDIES FOR SIDIS PROCESSES AND MAKING A RELATED EVENT GENERATOR FOR THE PROPOSED SOLID EXPERIMENT

In the upcoming years, highly accurate electron scattering experiments will be carried out in the 12 GeV Jlab program [66], which will provide unique opportunities for breakthrough studies of nucleon structure,

based upon precision measurements of single and double spin asymmetries from semi-inclusive deep-inelastic-scattering (SIDIS) experiments to probe the partonic structure in momentum space, by utilizing detectors with high luminosity in combination with large acceptance. The Solenoidal Large Intensity Device (SoLID) will be such a high luminosity and large acceptance tool [67], very well adapted for studies of nucleon structure.

It is well known that one of the important sources of systematic uncertainties in SIDIS experiments is the QED RC. For example, the systematic uncertainties on asymmetry measurements for SIDIS in SoLID are estimated to be 2-3% due to the RC effect. Currently, we are developing a new standalone event generator for polarized SIDIS including the finite mass of the lepton and QED RC following the calculations of Ref. [68]. This paper shows exact analytical expressions for the lowest order RC to SIDIS of polarized particles, obtained in the most compact, covariant form convenient for a numerical analysis. The calculations of RC have been performed in a model-independent way that involves constructing and using the SIDIS (and exclusive) hadronic tensor containing the eighteen SIDIS (and exclusive) structure functions. The SIDIS structure functions can be expressed in terms of Fourier-transformed transverse momentum-dependent parton distribution functions and fragmentation functions. The model-independent RC calculations in [68] include the contributions of radiated SIDIS processes with loop diagrams, and the contribution of the exclusive radiative tail.

Configurability and extensibility are primary goals for the development of the aforementioned event generator, including providing either weighted or unweighted events, using approximations to the cross section for performance (such as the ultrarelativistic approximation), and using user-provided SIDIS structure functions. The generator software is being developed in parallel between a Mathematica prototype and the final C++ library. The C++ library will be developed with a focus on performance, particularly with regard to the evaluation of high-dimensional integrals from the SIDIS structure functions and partonic degrees of freedom. Pending further investigation, either the FOAM library or a Markov Chain Monte Carlo method [69] will be used for evaluating these integrals and providing unweighted events to the users. This new generator will be implemented into comprehensive SoLID SIDIS full simulations.

This work is supported in part by the U.S. Department of Energy under Contract No. DE-FG02-03ER41231.

Radiative corrections for MUSE

F. Myhrer, P. Talukdar, V. C. Shastry, U. Raha

Introduction Determinations of the proton’s r.m.s. radius have produced results which are not consistent with earlier results [70]. The proton radius puzzle refers to the contrasting results obtained between the proton’s electric charge radii extracted from the Lamb shift of muonic hydrogen atoms and those extracted from electron-proton scattering measurements (see, e.g., Refs. [71, 72].) In order to resolve this issue, a number of newly commissioned experiments are underway, along with proposals of redoing the lepton proton scattering measurements at low momentum transfers. The latter includes the MUon proton Scattering Experiment (MUSE) [37, 73]. The MUSE collaboration proposes to measure the elastic differential cross sections for $e^\pm p$ and $\mu^\pm p$ scattering at very low momentum transfers, and aims for an r.m.s. radius error of about 0.01 fm. However, the lepton beam momenta considered by MUSE are of the order of the muon mass [37, 73]. A particular concern is therefore the standard radiative correction procedure, see, e.g., Refs. [2, 38]. The inelastic bremsstrahlung process is an integral part of the lepton-proton elastic scattering, and is a source of uncertainty for an accurate determination of the value of the momentum transfer Q . The influence of the in principle detectable ”hard” photon bremsstrahlung spectrum is discussed in earlier publications, e.g. [41] and will not be considered. We just note that in order to determine the proton charge radius, the data analysis necessarily need to correct for this inelastic radiation process. We will concentrate on the emitted very *soft* bremsstrahlung photons in order to evaluate the complete radiative corrections to the elastic lepton-proton scattering $\delta_{2\gamma}$. This radiative correction has been evaluated in a model independent way using *Heavy Baryon Chiral Perturbation Theory* (χ PT) to next-to-leading order (NLO)[74]. We find the observed differential cross-section to be

$$\left[\frac{d\sigma_{el}^{(NLO)}(Q^2)}{d\Omega'_l} \right]_\gamma = \left[\frac{d\sigma_{el}(Q^2)}{d\Omega'_l} \right] (1 + \delta_{2\gamma})$$

We note that the electron behaves relativistically whereas the muon mass is not ultra-relativistic at these low MUSE

energies, see Ref. [74] for complete discussions.

Radiative Corrections to Low Energy Lepton Scattering At low energy scattering hadrons are the relevant degrees of freedom, the dynamics is governed by chiral symmetry requirements. χ PT is a low-energy hadronic effective field theory (EFT), which incorporates the underlying symmetries and symmetry breaking patterns of QCD. In χ PT the evaluation of observables follow well-defined chiral power counting rules, which determines the dominant *leading order* (LO) contributions, as well as the NLO and higher order corrections to observables in a perturbative scheme. For example, in χ PT the proton’s r.m.s. radius enters at a chiral order where one encounters pion loops at the proton-photon vertex, e.g., Ref. [75]. Furthermore, χ PT naturally includes the photon-hadron coupling in a gauge invariant way.

We treat the leptons relativistically, i.e. the lepton current is $J_l^\mu(Q) = e\bar{u}_l(p')\gamma^\mu u_l(p)$, where the four-momentum transfer to the proton is $Q = p - p'$, and the lepton mass m_l is included in all our expressions. The hadronic current is derived from the χ PT Lagrangian. The proton mass, m_p , is large, of the order of the chiral scale $\Lambda_\chi \sim 4\pi f_\pi \sim 1$ GeV, where $f_\pi = 93$ MeV is the pion decay constant. The expansion of the Lagrangian in powers of m_p^{-1} is an integral part of χ PT. The *dynamical* m_p^{-1} corrections arise from the NLO photon-proton interaction of the Lagrangian. In particular, the anomalous magnetic moments of the nucleons and the Pauli form factor enter in a natural way in the χ PT formalism at NLO.

We consider all photon loops in χ PT including the *two-photon* exchange contributions. When necessary we invoke the *soft* photon approximation. Furthermore, the UV and IR divergences are treated using the dimensional regularization scheme, see Refs. [74, 76] for details. We find, for example, that the LO muon radiative correction goes through zero at some low Q value leaving the NLO corrections to be the dominant one around this particular Q value. We remark that at low energy χ PT we need a systematic improvement of the ”radiative tail” following Ref. [77].

Radiative Corrections in SIDIS: Current Status and Perspectives

Igor Akushevich and Alexander Ilyichev

The model-independent radiative corrections (RC) to the semi-inclusive deep inelastic scattering (SIDIS) cross section contain four principal contributions: i) loop diagrams and soft photon radiation (indistinguishable because of the infrared divergence), ii) hard photon emission with semi-inclusive process, iii) hard photon emission with exclusive process, and iv) multiple soft photon emission. Each process is calculable exactly and the use of exact formulae in the RC procedure of experimental data with estimating systematic error due to RC is the gold standard in data analyses of modern experiments on lepton-nucleon scattering. By “exact” we understand the formulae allowing to exactly reconstruct the leading and next-to-leading terms at least. Various approximations to exact formulae are possible but their accuracy can be estimated only based on comparison to the exact formulae. Our experience in analyses of data in deep inelastic scattering (DIS) tells us that the difference between estimates based on exact and approximate formulae can reach 100% and strongly depends on a kinematical point. Possible (reasonable) approximations used in literature and data analysis practice include: i) soft photon approximation, ii) leading log approximation, iii) peaking approximation, iv) Compton-peak approximation, and v) using different Monte Carlo generators (e.g., RADGEN [78]). The soft photon approximation is very convenient because RC is factorized at the Born cross section and completely cancels in spin asymmetries, but is wrong because of hard photon emission that cannot be neglected even in experiments with much poorer accuracies comparing to SIDIS experiments in JLab. The leading log (and peaking) approximation could estimate RC from hard photon with semi-inclusive process but is not applicable for the radiative tail from exclusive peak (or simply exclusive radiative tail). The Compton-peak approximation was good for the elastic radiative tail in DIS, but our estimates show that it will not work even for the exclusive radiative tail.

The methodology used in experimental laboratories for accounting of radiative effects in SIDIS was basically a generalized version used for inclusive DIS studies, typically using RADGEN generator [78] combined with different full event generators, like PYTHIA[79], LEPTO[80], PEPSI [81]. That approach, while providing some estimates for RC, is inconsistent, as RADGEN itself contains only some version of DIS structure functions (SFs), and LUND base generators, completely ignore all kind of spin-orbit correlations. Unfortunately this approach is not applicable for analysis of azimuthal asymmetries in SIDIS, because key parts of the cross section responsible for $\cos(\phi_h)$ and $\cos(2\phi_h)$ do not appear in RADGEN. Therefore, the correct cross section of radiated photon cannot be reconstructed using an approach

involving pure-DIS Monte Carlo generators of RC. Precision studies of azimuthal moments in SIDIS will require a completely new methodology for accounting of radiative effects in SIDIS, taking as input some set of realistic SFs describing all relevant moments for specific observables under study. The extraction of an azimuthal moment of interest, thus, will require a full extraction of all azimuthal moments contributing to the SIDIS cross section for a given configuration of beam and target polarizations.

Therefore, the only way to provide a reasonable calculation of RC is based on the exact formulae for RC in SIDIS. Such formulae have to provide contributions from all 18 (5 spin-independent and 13 spin-dependent) SFs of SIDIS [82] as well as all respective terms in the exclusive radiative tail. Currently, the RC to the SIDIS cross sections and polarized asymmetries can be calculated using POLRAD 2.0 [83] and HAPRAD 2.0 [84]. In POLRAD 2.0, the RC cross section is calculated in terms of the parton distributions $f(x)$ and fragmentation functions $D(z)$, i.e., the simple quark-parton model is assumed. RC for unpolarized cross section and polarized part of the cross section are calculated, but no the exclusive radiative tail is separately calculated. Integration over p_t and ϕ_h is assumed, i.e., the RC to the three-fold cross section is calculated: $d\sigma/dx dy dz$. Several models for the parton distributions and fragmentation functions are implemented. In HAPRAD 2.0, RC to the five-dimensional cross section $d^5\sigma/dx dy dz dp_t^2 d\phi_h$ are calculated. The contribution of the exclusive radiative tail was implemented as a separate term that uses SFs for exclusive processes. Thus, although these codes are not applicable to polarized SIDIS or contain limitations that make them inapplicable in data analyses of modern SIDIS experiments, their use allows us to develop our expectations on the size of the RC: i) x and Q^2 -dependences are similar to what we have in DIS; ii) RC go down with increasing z , e.g., RC factor can change from 1.05 to 0.85 between $z=0.2$ and 0.8 for the same x and Q^2 : the z -dependence of RC is generated by decreasing the phase space of radiated photon with increasing z ; iii) p_t -dependence is strong: RC can increase by a factor of 2 or more for very high p_t : both semi-inclusive and exclusive processes have large RC for large p_t ; iv) RC to ϕ_h -dependence can be large (RC generate new ϕ_h -dependence and therefore new observables like $\langle \cos(3\phi_h) \rangle$ that are exactly zero at the Born level); and v) RC from the exclusive radiative tail has its own dependence on kinematical variables and can give a high contribution especially as small M_x^2 (e.g., RC factor is 0.95 and 1.4 without and with the exclusive radiative tail for $M_x^2=1.5$ GeV² or 1.05 and 1.3 for $M_x^2=3.0$ GeV²) and for high p_t . Radiative corrections in the polarized case are largely unknown. From our experience in DIS, we ex-

pect similar patterns of RC and their larger size for the polarized part of the cross section. The effect is strongly dependent on the model for SFs. The strong model dependence can be partly addressed by applying the RC iteration procedure of experimental data. An illustration of possible effect of RC in unpolarized case shows that terms from SFs responsible for ϕ_h -dependence can significantly contribute to the RC cross section with generation of higher harmonics that are significantly large in magnitude. For example, for kinematical point $E_{beam}=10$ GeV, $Q^2=2.5$ GeV², $x = 0.25$, $z = 0.2$, and $p_t=0.7$ GeV, the estimate of $\langle \cos(3\phi_h) \rangle$ is about 5%.

Recently, we completed the calculation of RC to SIDIS with longitudinally polarized lepton and arbitrary polarized nucleon [68]. The exact calculation of RC for the SIDIS cross section contained contributions from all 18 SIDIS and 18 exclusive SFs and required derivation of the hadronic tensor for both the SIDIS and exclusive cross sections in the covariant form. Specifically, the stages of the theoretical calculation and practical implementation included the steps: i) elaborating the covariant hadronic tensor of SIDIS based on developments of the theoretical groups of Aram Kotzinian [82], Peter Mulders [85] and Alessandro Bacchetta [86]; ii) calculating the SIDIS cross sections using the elaborated hadronic tensor and compare analytic expressions for the Born cross section between the results obtained by researchers of these groups and understand possible discrepancies; iii) calculating the coefficients from convolution of the leptonic tensor involving RC with tensor structures from the hadronic tensor; and iv) evaluating the loop effects and extraction and cancellation of the infrared divergence using the covariant approach of Bardin and Shumeiko [87]. The next steps could include implementation of the formulae to a code for numeric analyses, estimation of accuracies of most popular approximations, investigation of the model dependence of the RC, and identification of the kinematical regions where uncertainty in SFs could result in significant effect on RC. Note, any Monte Carlo generator that is required to reasonably simulate RC in SIDIS experiments must be based on the exact formulae. Therefore, we also intend to develop a Monte Carlo generator that will simulate the channel of scattering (non-radiative, radiative SIDIS, and radiative exclusive scattering) and the kinematical variables of the radiated photon. The strong model dependence can be partly addressed within a re-

alistic RC procedure of SIDIS experimental data that should involve an iteration procedure in which the fits of SFs of interest are re-estimated at each step of this iteration procedure. This procedure could be defined with and without involving Monte Carlo generator. Independently of whether MC is involved the procedure has to include the following steps: i) fitting the SIDIS SFs to have the model in the region covered by a SIDIS experiment; ii) using experimental data or theoretical models to construct the models in the regions of softer processes, resonance region, and exclusive scattering, iii) checking that the constructed models provide correct asymptotic behavior at the kinematical bounds (Regge limit, QCD limit); iv) jointing all the models to have continuous function of all four variables in all kinematical regions necessary for RC calculation; v) implementing this scheme in a computer code and defining an iteration procedure; vi) implementing the procedure of separation SFs if several SFs are measured in an experiment; vii) constructing the models for other SFs are if necessary (e.g., unpolarized SFs when spin asymmetries are measured); viii) paying specific attention to exclusive SFs, because the exclusive radiative tail is important (or even dominate) in certain kinematical regions; and ix) paying specific attention to p_t dependence because RC is too sensitive for p_t model choice.

In summary, newly achieved accuracies in Jlab and new physics studied at Jlab require paying renewed attention to RC calculations and their implementation in data analysis software. Although the theoretical calculation of RC to SIDIS is performed, current codes for computation of RC to SIDIS are not applicable to polarized SIDIS or contain limitations that make them inapplicable in data analyses of modern experiments. Lack of reasonable models for all 18 SIDIS SFs is the main obstacle in creating a workable code based on the exact formulae. We expect sensitivity of the results for RC to specific assumptions used for constructing SIDIS SFs. Therefore, broad discussion and efforts of theoreticians and experimentalists are required to complete parameterizations of all SIDIS SFs as well as SFs in resonance region and exclusive SFs. The iteration procedure with fitting of measured SFs and joining with models beyond SIDIS measurements at each iteration step looks the better solution for specification of RC procedure of SIDIS experimental data.

New Physics at Low Energies and the Conceivable X17 Boson: Perspective on Atomic Transitions and Scattering Experiments

Ulrich D. Jentschura

Introduction.—At the moment, it seems that the proton radius puzzle could be solved by experimental considerations alone, after new high-precision spectroscopic measurements have revealed that the (certain hyperfine components of the) hydrogen $2S-4P$ frequency interval [88] and the $2S-2P$ Lamb shift [89] are in agreement with the new, lower value of the proton radius [53, 90, 91].

On the other hand, the scattering experiment [71], which led to a roughly 5% larger proton radius as compared to Refs. [53], constitutes an exemplary accomplishment in terms of diligence in both planning and execution. Furthermore, several high-precision spectroscopy measurements of the Paris group (e.g., Refs. [92, 93] and also the new measurement [94]) are in agreement with the “larger” proton radius.

In view of this interesting situation, we believe that, even if the proton radius puzzle should be solved based on a reconsideration of experimental aspects alone, one should keep in mind the possibility of the emergence of “New Physics” at the low-energy scale, possibly visible in high-precision spectroscopy and scattering experiments.

One curious observation, recently made at the ATOMKI Institute of Nuclear Physics in Debrecen, Hungary, concerns the possible existence of a hitherto unobserved 17 MeV gauge boson, termed the X17 boson [95–97], which could modify scattering cross sections and high-precision spectroscopic measurements of simple atomic systems.

The case for muonic bound systems.—In two recent papers [98, 99], we have analyzed the possible effect of the X17 gauge boson on transition frequencies in simple atomic systems. One of the general conclusions has been that in bound systems where the orbiting particle is an electron, the virtual X17 exchange cannot easily be distinguished from nuclear effects, because the reduced Compton wavelength of the X17 is commensurate with the nuclear radius. We recall that both the nuclear size (of the order of one fermi) as well as the reduced Compton wavelength of the X17 (of the order of about ten fermi, see Ref. [98]) are much smaller than the Bohr radius.

The situation is fundamentally different in muonic bound systems. Namely, in muonic systems, the effective Bohr radius is smaller than in electronic bound systems by roughly a factor of 100, and thus, the overlap of the X17-induced Yukawa-type potentials with the atomic wave function is much larger in bound systems where the orbiting particle is heavier than the electron.

It turns out that the effects induced by the X17 are still very elusive when it comes to measurements of the Lamb shift [98], even in muonic bound systems. This is because of the small coupling parameters of the X17, which are much smaller than the QED fine-structure constant, the

latter being the coupling parameter of quantum electrodynamics (QED) (see Refs. [100–102]).

However, in the hyperfine splitting, the situation is different: The magnetic field of the nucleus generates the Fermi splitting [103], which, for S states, is given as the expectation value of a Hamiltonian proportional to a Dirac- δ in coordinate space. From this observation alone, it is clear that hyperfine effects correspond to short-range interactions, and that the effect of the X17 will be much more visible in hyperfine transitions as compared to other transitions which involve a change in the principle quantum number, or the angular-momentum quantum numbers (ℓ and j) of the orbiting particle.

According to Eqs. (61a) and (61b) of Ref. [99], the effect of the X17 enters the hyperfine splitting of muonic deuterium already at the relative level of 10^{-6} , expressed in terms of the Fermi splitting. Hyperfine transitions among P states suffer much less from uncertainties due to nuclear structure, due to the small overlap of the P state wave function with the nucleus. The effect of the X17 on P states shifts the transition frequency by a relative fraction of a few parts in 10^7 . Under a moderate increase in the theoretical accuracy connected with nuclear-structure effects, the X17 might thus be visible in muonic deuterium [99].

Let us also consider the “purest and most interesting QED system imaginable”, namely, true muonium (the bound system consisting of a muon and its antiparticle). The designation is recalled from memory, from conversations with the late Professor Gerhard Soff [104], who advocated and advised theoretical work on this system [105, 106]. In true muonium, the effects of the X17 on the hyperfine splitting are even more pronounced, entering the S state hyperfine splitting at a few parts in 10^6 [see Eq. (69) of Ref. [99]]. A very moderate increase in the theoretical precision for hadronic vacuum polarization effects [107] could thus make the X17 visible in true muonium.

Implications for Scattering Experiments.—We have singled out, above, the case of muonic deuterium as opposed to hydrogen, because one of the two favored theoretical models for the X17 [101, 102] predicts a “protophobic” X17 which would, to a good approximation, only couple to neutrons, not protons.

In scattering experiments, one would thus expect the X17 to produce a slight “halo” in muon-deuteron scattering experiments, which can be distinguished from the nuclear-size effect in the range of momentum transfers about 17 MeV and larger.

For the other favored theoretical model of the X17 (Ref. [100]), which involves a conjectured pseudoscalar virtual particle, the interaction is spin-dependent on the

level of in the leading order [see Eqs. (19) and (23c) of Ref. [99]], and is thus visible, to good approximation, only in the spin-resolved, differential cross section as opposed to the total scattering cross section.

These general observations on scattering experiments would need to be substantiated by more concrete theoretical calculations and feasibility studies. The effect of the X17 boson on scattering experiments could provide grounds for additional highly interesting theoretical investigations and experiments.

Proton size puzzle and new effects.—On the occasion, in addition to conceivable effects mediated by the X17 boson, we may discuss other conceivable new effects to be discerned in low-energy high-precision experiments. Indeed, it may be premature at the current stage to completely discard other questions that surround the very recent, conflicting results on the proton radius [53, 94].

In particular, one might investigate the following question. The proton wave function is an eigenstate of a Hamiltonian, which contains the sum of the quantized electromagnetic interaction (quantum electrodynamics, QED) and the quantized strong interaction (quantum chromodynamics, QCD). The primary particle content of the proton is given by the three valence quarks. However, it is well known that the contribution of additional “sea” quarks also forms part of the proton wave function, in view of the nonperturbative character of the strong interaction. Now, it can be checked by elementary calculations that the electric field strength inside the proton reaches values close to Schwinger’s critical field at which the vacuum “sparks” and electron-positron pairs are created. It is thus conceivable and in fact, also inevitable [108] that the proton wave function also contains light “sea” fermions (primarily electron-positron pairs, with muon pairs being kinematically suppressed in view of the larger mass). The sea leptons are nonperturbative in the sense that they belong to the initial state of the proton in the scattering experiment and thus are not comprised in the proton polarizability contribution to scattering, the latter having contributions from additional loops with electron-positron pairs, which, however, have to be excited perturbatively during the scattering

(see Figs. 2 and 3 of Ref. [109]). If the light sea-fermion effect exists, then the proton radius would have to come out larger in electron scattering than in muon scattering, because the virtual annihilation can only happen within one and the same particle generation. This conjecture would be consistent with the findings of a 1969 experiment [110]. The problem has been discussed further in Refs. [111, 112]. With highly conflicting results on the proton radius [53, 94] and with reference to the seasoned experiment [110], we believe that the proton radius puzzle will need to be explored further.

Conclusions.—For many decades, low-energy additions to the Standard Model have been explored without any imminent breakthroughs in sight. High-precision spectroscopy and scattering experiments have looked for such additions in tiny deviations of theory and experiment, but so far, have found none. One should perhaps not forget that conjectures have been formulated for additions to the structure of the proton (light sea fermions, Refs. [109, 112]) which suggest that the proton radius puzzle could open the window to new and interesting effects. At the moment, it could appear that the proton radius puzzle is explained based on experimental advances alone [53, 88, 89], but this finding would probably need to be confirmed by additional experiments before a final line can be drawn. In addition to increasing the accuracy of theoretical predictions even further, a significant motivation for the experiments have been the hunt for tiny fifth-force interactions, which could be visible in the deviations of theory and experiment. The putative observation of the X17 boson [95–97] provides us with a candidate model that should be explored further, with a possible impact on high-precision spectroscopy and scattering experiments [99].

Finally, in view of recent, mutually contradictory results on the proton radius [53, 88, 89, 94], the hope is expressed that future experiments will be consistently evaluated. This hope is being formulated taking into account a possible non-universality of electron-proton versus muon-proton interactions [109, 110, 112].

Acknowledgments.—Support from the National Science Foundation (Grant PHY–1710856) is being gratefully acknowledged.

Summary EIC MC activities

Markus Diefenthaler

Markus Diefenthaler presented activities by the EICUG Software Working Group (SWG). The SWG has participated in the call for Expressions of Interest (EoI) by the EICUG and asked the community to present software needs for the EIC and how to meet this needs:

- **Requirements** What software needs for EIC Software would you like to highlight now, in a few years, and for the completion of the EIC project?
- **Technologies & Techniques** What software technologies and techniques should be considered for the EIC?
- What resources can your group contribute?

Based on the community input, the SWG submitted a Software EoI that will evolve towards a work plan, setting priorities for the next years and goals for the next decade. The SWG has reviewed Monte Carlo event generators (MCEGs) for ep and eA processes and discussed their requirements and developments for the science program at the EIC.

For the preparation of the TDR, the SWG will maintain a collection of MCEGs that are used in the EICUG and are validating them against existing DIS data. It will provide an online catalog of MCEGs where the community can select MCEGs and find documentation, valida-

tion plots, and examples on how to use the MCEG with existing EIC Software. The MCEGs will be fully integrated in the workflows for physics and detector simulations. Comparison to H1, ZEUS, and COMPASS measurements are being used to validate the MCEGs. For the MC-data comparison, the SWG is utilizing the RIVET tools as recommended by the worldwide MC community.

For the completion of the EIC project, the SWG will define with the community what part of the MCEG collection can be substituted and what part needs to be preserved for the EIC. It will make the necessary changes to the legacy MCEGs to ensure their future compatibility, e.g., adding HEPMC3 as output format and integrating them in the RIVET workflow. At the same time, the SWG will work with PARTONS and other initiatives to integrate new and upcoming MCEGs in the MCEG collection. The SWG will collaborate with the worldwide MCEG community on a global DIS tune based on our validation work. Merging of QED and QCD effects in MCEGs and correcting for these effects in the analysis will be essential. Please consider joining the SWG efforts and help with your expertise.

The software development will build upon the infrastructure of the EICUG, including the GitHub organization and the GitHub website. Please consider storing (or mirroring) your source code and examples, e.g. on unfolding algorithms, in the EICUG GitHub organization (<https://github.com/eic>).

Second-Order Radiative Corrections for ep Scattering

Hubert Spiesberger

First order radiative corrections for electron proton scattering have been known to be large since long. They are enhanced by large logarithms of the ratio of the momentum transfer Q^2 and the electron mass m_e , $\ln(Q^2/m_e^2)$, due to radiation of photons collinear with the incoming or scattered electron. In addition, a strong enhancement of radiative corrections is possible due to the fact that the energy carried away by a radiated photon leads to a shift of the momentum transfer to small values. This radiative tail is particularly important in inelastic scattering at large inelasticity y , reaching corrections in the order of 100 %, but is also important for elastic scattering.

One should therefore expect that the suppression due to additional powers of $\alpha/2\pi$ of corrections beyond the first order is counteracted by the presence of additional powers of a large logarithm. Kinematic cuts on the observed scattered electron or on the allowed photon energy can lead to an additional enhancement. Radiative corrections therefore depend strongly on the details of the experiment and should be studied with the help of Monte Carlo event generators which can simulate the experimental conditions.

Leptonic corrections are the dominating contribution to higher-order corrections. Since this contribution is gauge invariant by itself, it can be calculated separately. It is described by Feynman diagrams where photons are attached in all possible ways to the lepton line, see Fig. 10. At second order one has to take into account two-loop diagrams, one-loop corrections to radiative scattering, and diagrams for the emission of two photons.

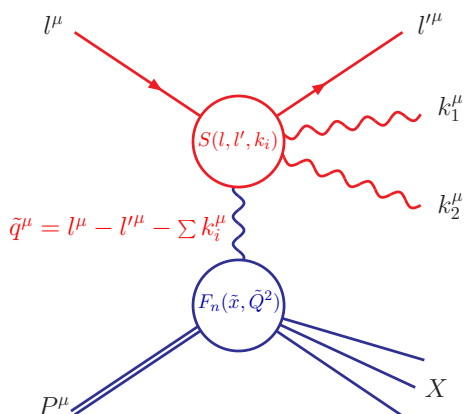


FIG. 10. Leptonic radiative corrections to lepton-proton scattering can schematically be described as a convolution of a radiator function $S(l, l', k_i)$ due to photon emission from the lepton line with structure functions or form factors $F_n(x, Q^2)$ describing the hadron structure. The radiator function S includes δ -function terms from loop corrections.

Infrared divergences, present in each part separately, are cancelled when real and virtual corrections are combined. Details of the calculation can be found in Ref. [113] (see [114] for an alternative approach).

In the limit of vanishing photon energy, i.e. in the soft-photon limit, higher-order corrections can be estimated by exponentiation. Also logarithmically enhanced contributions due to hard collinear photons can be calculated approximately. A convenient approach is based on the QED analog of parton splitting functions known from QCD, see for example [115, 116]. These leading-log calculations are based on the assumption that radiation is strictly collinear, i.e. on the peaking approximation. Forthcoming high-precision measurements, however, require a calculation which goes beyond these approximate approaches.

As an example we show in Fig. 11 the cross section for radiative ep scattering, i.e. with an additional photon in the final state [113]. After integrating over the photon phase space, this contributes a correction of order $O(\alpha)$ to elastic ep scattering. We have chosen the kinematic variables at values which are relevant for the P2 experiment at MESA, Mainz, [117] i.e. an electron beam energy of $E = 155$ MeV and a scattering angle of 35° . We have integrated over the photon energy imposing a lower cut-off $E_\gamma \geq 10$ MeV. The graph exhibits two prominent peaks, one at small angles where the photon is emitted into a direction close to the initial electron, and one at 35° where the radiated photon is close to the scattered electron. Radiative scattering appears with a substantial tail to angles far away from the incoming or scattered electron. It is obvious that a peaking approximation, based

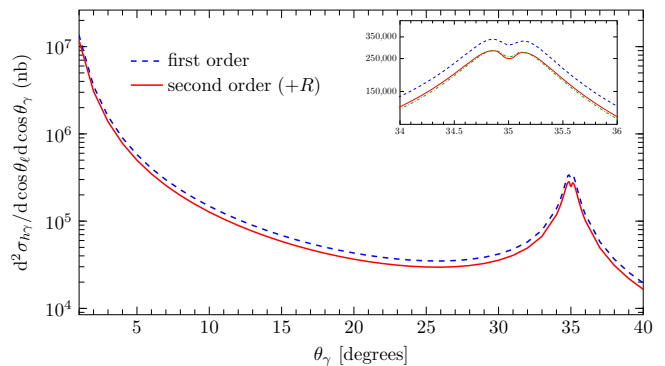


FIG. 11. Differential cross section for radiative ep scattering as a function of the photon emission angle at leading order (blue dashed curve) and including $O(\alpha)$ corrections (red full curve). The beam energy is $E = 155$ MeV and the electron scattering angle is fixed at $\theta_e = 35^\circ$. The radiated photon is allowed to have an energy between 10 MeV and the kinematic maximum.

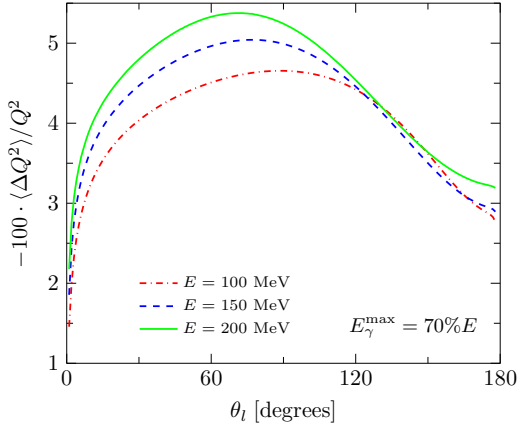


FIG. 12. Average relative shift of the momentum transfer (in percent) for three values of the electron beam energy, assuming that a radiated photon can take away up to 70 % of the beam energy.

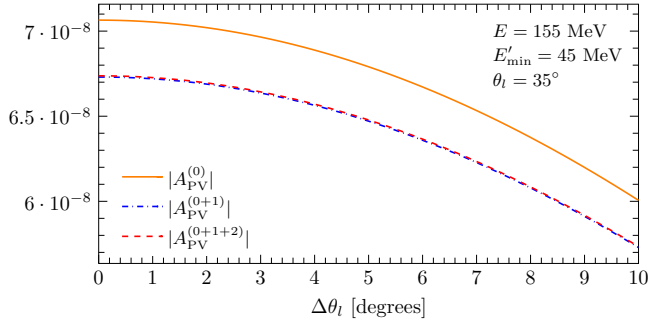


FIG. 13. The parity-violating asymmetry for elastic ep scattering of polarized electrons at the Mainz P2 experiment. The large corrections are due to the shift of Q^2 by photon radiation. Second-order corrections are small in this case.

on the assumption that radiation is strictly collinear, is not appropriate if one requires high-precision.

For an interpretation of ep cross section measurements in terms of structure functions or form factors, a precise knowledge of the momentum transfer is needed. If a radiated photon stays unobserved, the true momentum transfer to the proton can not be calculated from the scattering angle of the electron. This kinematic effect can amount to several percent, as shown in Fig. 12. It is important for the extraction of the weak mixing angle from a measurement of the parity-violating helicity asymmetry, as planned at the P2 experiment at MESA in Mainz [117]. Figure 13 shows the result of a calculation at leading order, as well as one including first-order and second-order corrections. In this case, one finds only small corrections at order $O(\alpha^2)$.

While the theoretical treatment of leptonic QED radiative corrections is well established, uncertainties remain when hadronic effects come into play. A full calculation will have to include also corrections due to photon radiation from the hadron side, as well as lepton-hadron interference effects combined with two-photon exchange contributions. They introduce an additional model dependence since they require knowledge of the hadron structure beyond the elastic form factors. These hadronic corrections are expected at the level of fractions of a per mille, much smaller than the leptonic corrections, but a verification of these expectations is needed for future high-precision measurements.

Higher-order calculations of RC for ep and Moller scattering

Stan Srednyak

Recently, the world value of the charge radius of the proton, as measured in ep collisions, was reconsidered [118]. This experiment was motivated by the previous measurement of this quantity in muonic hydrogen spectroscopic experiment [119]. Although at the moment there seem to be less disagreement between the two types of measurements [118] (after correcting the world value that corresponds to ep type measurement), this experiment lead physicists to reconsider theoretical background on which the interpretation of the data from these experiments is based. The conclusions are threefold. First, the bound state equation that was used for two loop computation [70, 120–122] for spectrum must be reconsidered because there are no first principles that substantiate this equation beyond one loop order. Second, on the scattering side, there are two photon exchange processes whose contribution can only be estimated, rather than calculated precisely [49, 123, 124], because currently theory does not provide means to evaluate the matrix elements of non local operators. Third, both these computations are very challenging from mathematical point of view, and the field would benefit greatly from the development of mathematical tools to facilitate these computations.

Extraction of the proton charge radius from spectroscopy experiments is based [70, 120] on the proportionality of the Lamb shift to this radius. This calculation is based on the Bethe-Salpeter equation. There is no explicit closed form solution to this equation. An approximation scheme (NRQED) was developed [120, 121, 125] for systematic extraction of terms of different order in $\alpha, \log(\alpha), m/M$. It is the expressions obtained by this scheme that are used to extract r_p from experimental data [70]. It is not the direct prediction of the Bethe-Salpeter equation that are used, but rather the results of the approximation scheme. There is little doubt that the terms in this scheme were extracted correctly, as this computation was checked by multiple groups (see [70, 120–122] and refs therein). Therefore, it is not the calculation that has to be reconsidered, but the basic principles on which this computation is based. The reconsideration must be twofold. First, it is known [126–128] that it is very hard mathematical problem to formulate gauge invariance in theories with multi-local terms, such as bound state equations. These equations must be functional, directly formulated in the full Hilbert space of the theory that involves towers of virtual particles. Unfortunately, activity in this direction was rather limited in the recent years [126, 127, 129], perhaps because it is very difficult to solve resulting equations even approximately (we wish to remind the reader that one-loop computation of leading terms to Bethe-Salpeter was completed [130] only after forty years after the importance of this problem was recognized [131]. This

equation is a toy model for the true functional equations for bound states.) Therefore, to make progress in this field, more resources should be allocated to the development of mathematical methods for the solution of such equations. Such methods would include, for example, the theory of hypergeometric functions on symmetric spaces [132, 133] (see more below).

Extraction of proton charge radius from ep scattering experiments must be accompanied by the evaluation and subtraction of radiative corrections to scattering. This problem is well defined except for the two-photon exchange process, which is currently model dependent. In PRad [118], this correction was only estimated. Therefore, to advance the interpretation of the results of PRad I and the reduction of error bars on r_p in this experiment, a new calculation of the radiative corrections is necessary. Moreover, it is desirable to advance these calculations to two loop order to match the accuracy on the spectroscopy side. This is a very difficult problem, as clearly recognized by the experts in the field [134–136].

The problem of evaluating two-photon exchange contribution is a fundamental one, drawing attention for long time (see the review [49] and refs therein, and modern [123, 124]). However, all these papers aim either at estimation of this effect (for example, by using dispersive methods [44] or model dependent vertices [124]) or extraction of parameters form e.g. charge asymmetry experiments [137]. The problem of evaluating this contribution in continuum QCD is largely considered intractable. It is related to the problem of finding the bound state equations for gauge theories and solving them at strong coupling. Although clearly inaccessible at this point, it draws attention to the development of powerful mathematical methods suitable for the solution of functional partial differential equations, and for systematic analysis of such equations. This latter research can be very fruitful in our opinion, as we detail later.

The evaluation of one loop corrections to ep scattering has been considered in many papers (see [68] and refs. therein). Extending this success story beyond one loop probably will lead to a disappointment because the corresponding calculations are very difficult [134–136]. The long standing problem here consists in the development of suitable mathematical tools for the evaluation of multi-loop integrals. There are many groups working in this direction. Let us mention only a few of them. In [138, 139], two-loop sunrise was investigated and it was shown that it leads to a new class of functions beyond the class of polylogarithms - so-called elliptic polylogarithms. There are deep connections with arithmetic algebraic geometry and the theory of motives [140]. General approach to multidimensional integrals was formulated long time ago in mathematical literature [141]. There are some

problems in adapting this approach to the physical situation, the main of them being the understanding the complicated geometry of singularity divisor of Feynman integrals. This approach has been pursued by the author [142], and it is hoped that it can lead to concrete numerical schemes suitable e.g. at two-loop order. This approach lead to the representation of Feynman integrals in the form

$$J_a = \sum L_i^{\alpha_{a,i}} g_{a,i}(q_p) \quad (5)$$

where L_i are Landau polynomials and $g_{a,i}(q_p)$ are analytic functions depending only on the coordinates on the locus $L_i = 0$, for which a similar expansion holds. The coefficients in this expansion can have poles in $d - 4$. Therefore, the function of all the kinematical invariants can be decomposed into a tower of functions depending on progressively less variables. It is still a difficult problem to evaluate the coefficients in this expansion. One of the approaches to this problem involves pull-back of holonomic D-modules and b-functions [143]. The general paradigm of application of this approach consists in 1) finding expressions for the Landau polynomials 2) finding the set of master integrals 3) finding the exponents $\alpha_{a,i}$ for each Landau polynomial and each master integral 4) stratification of the parameter space by multiple intersections of Landau polynomials 5) expanding iteratively master integrals and coefficient functions $g_{a,i}$ into the Gamma-series of the above type. Each of these steps is non trivial. For example, even the evaluation of Landau polynomials leads to expressions of very high degree, as in general it involves determinants of discriminantal complexes [144, 145]. The next problem is the description of singularities of their intersections. This problem is not solved for two loop integrals (it probably leads to a set of interesting arithmetic varieties). Although it is possible to use the Landau polynomials as coordinates on the space of kinematic invariants, it may be advantageous to study different algebro-geometric models of this space, for example, resulting from various blow-ups of this space [146]. The problem of finding analytic expression for sections of flat $GL(n, C)$ bundles has also been considered from moduli point of view [147] (so-called Higgs bundles in the case of Riemann surfaces). Feynman diagrams correspond to very specific high dimensional representations of the fundamental group of the parameter space. Therefore, the question arises, how do these bundles correspond to points in the moduli space of general rank r bundles on the parameter space. The approach to this problem is provided by isomonodromy approach. Unfortunately, the isomonodromy theory is well developed only in the case of 1d parameter space, while we need it for multiple dimensions (already in 1d case, it is much more complicated when the Riemann surface is different from the Riemann sphere). Therefore, a very bold extension of the existing methods must be accomplished in order to set this problem on rigorous mathematical basis. A

typical result that one should strive for in this area may consist in classification of stratified spaces arising in on-shell 2-2 scattering, and classification of Pfaffian forms of regularly singular PDEs on such spaces.

Recent developments [140] substantiate the exciting realization that the multiloop integrals are in fact number theoretic objects. Number theory enters through the geometry of the singularity locus. There are number fields associated to particular multiloop diagrams. These number fields are generated by coordinates of zero-dimensional strata in the stratification by intersections of Landau polynomials. What is the physical meaning of this phenomenon (if any) remains to be explored.

As we mentioned, the development of continuum QCD will entail development of techniques to solve functional partial differential equations [126, 127, 129]. One of the simplest such equations is the following functional Laplacian

$$\int dx dy K(x, y) \frac{\delta^2}{\delta\phi(x)\delta\phi(y)} F[\phi] = 0 \quad (6)$$

for a given function $K(x, y)$. In the case of Bethe-Salpeter, this function involves 2-2 kernel (and thus, at one loop, dilogarithms) but as a toy model one can take $K(x, y) = 1/P(x, y)$ with a generic polynomial $P(x, y)$. Note that this equation is meaningful even in the case of 1d space. It is remarkable fact that the formal solution of this equation can be sought in the form of the series of the type eq. 5. I.e., before we resum the series, individual terms are flat bundles on a complement of the zero locus of several polynomials, that are generated by the original form of $K(x, y)$. Flat bundles provide a kind of universal class of functions which solve a variety of problems in QFT. Resummation will call for a wide extension of this function class. It will be necessary to consider the class of functions that have logarithmic singularities along a locus given by zero set of an entire function of the kinematic invariants. This is work in progress by the author.

The problem of continuum bound state formulation of QCD (and QED beyond one loop) leads to deep questions of the theory of functions of several complex variables. In particular, it is known that asymptotics at infinity (in x-space) of wave functions is exponential. This theory is well understood in 1d case [148], but it is much less understood in multidimensional case, as needed for physics [149–151]. What is clear at the moment is that a multidimensional analogy of Stokes phenomenon is involved in understanding multiparticle states. The question lies in the description of the class of function in which to seek for solutions. A broad class of functions is provided by so-called resurgent functions [152]. Remarkably, this same class shows up in the problems of quantum mechanics that involve chaotic phenomena [153]. As these are toy problems compared to the true bound state problems with radiative corrections, it is highly unlikely that it will be possible to avoid considering this broad function class.

Factorized approach to radiative corrections for inelastic lepton-hadron collisions

Jianwei Qiu

Introduction— We propose a new factorized approach to QED radiative corrections (RCs) in inclusive and semi-inclusive lepton-hadron deep-inelastic scattering (DIS), which treats QED and QCD radiation on an equal footing. The method allows the systematic resummation of the logarithmically enhanced RCs into factorized lepton distribution and fragmentation (or jet) functions that are universal for all final states. The new approach provides a uniform treatment of RCs for the extraction of parton distribution functions, transverse momentum dependent distributions, and other partonic correlation functions from lepton-hadron collision data [154].

Instead of treating QED radiation as a correction to the Born process [2, 155], which becomes increasingly difficult beyond inclusive DIS [68, 156, 157], we unify the QED and QCD contributions in a consistent factorization formalism. The new approach allows all collinear (CO) sensitive and logarithmically-enhanced photon radiation to be systematically resummed into factorized, either CO or TMD, universal lepton distribution functions (LDFs) and lepton fragmentation (or jet) functions (LFFs), or as QED modifications to the evolution of nucleon PDFs or TMDs. The remainder of the QED contributions are then insensitive to lepton mass $m_e \rightarrow 0$, and included in the infrared (IR) safe, perturbatively calculable hard parts, plus corrections suppressed by powers of m_e over the hard scale of the collisions. Calculating RCs is then replaced by determining the universal LDFs and LFFs, along with perturbative calculation of IR-safe QED corrections to the short-distance hard parts. With both QCD and QED factorization, the new framework provides a consistent and perturbatively stable strategy to extract PDFs and TMDs from lepton-nucleon scattering.

Inclusive lepton-nucleon DIS— In the absence of photon radiation from leptons, and dropping lepton and hadron masses, the inclusive cross section for lepton-nucleon DIS $e(\ell) + N(P) \rightarrow e(\ell') + X$, is given by

$$E' \frac{d\sigma_{\text{DIS}}}{d^3\ell'} = \frac{4\alpha^2}{s x_B y^2 Q^2} \left[x_B y^2 F_1 + (1-y) F_2 \right], \quad (7)$$

where α is the electromagnetic fine structure constant, and the kinematic variables are given by $s = (\ell + P)^2$, $Q^2 = -q^2 = -(\ell - \ell')^2 > 0$, $x_B = Q^2/2P \cdot q$, and $y = P \cdot q/P \cdot \ell$. The structure functions F_1 and F_2 can be factorized in terms of PDFs with corrections suppressed by powers of $1/Q^2$ [158]. The inclusive cross section (7) would then provide a clean probe of F_1 and F_2 [159–165].

In the presence of photon radiation, however, F_1 and F_2 are not direct physical observables. Without accounting for all photon radiation, the exchanged photon momentum q cannot be determined exactly, which impacts the extraction of PDFs. With the small m_e , photon radi-

ation could be enhanced by $\ln(Q^2/m_e^2)$, leading to large, but not precisely determined, RCs that are sensitive to kinematic variables such as x_B and Q^2 . The factorization approach proposed in Ref. [154], while unable to ensure the extraction of F_1 and F_2 , does nevertheless provide a perturbatively stable formalism for the reliable extraction of PDFs from inclusive DIS cross sections.

We consider the inclusive DIS cross section in Eq. (7) for a lepton scattered with a large transverse component $\ell'_T \gg \Lambda_{\text{QCD}}$ in the colliding lepton-nucleon frame. Applying the factorization formalism for single-hadron production at large transverse momentum in hadronic collisions [166] to lepton-nucleon scattering, the factorized DIS cross section can be written,

$$E' \frac{d\sigma_{\text{DIS}}}{d^3\ell'} = \frac{1}{2s} \sum_{i,j,a} \int_{z_L}^1 \frac{d\zeta}{\zeta^2} \int_{x_L}^1 \frac{d\xi}{\xi} D_{e/j}(\zeta) f_{i/e}(\xi) \\ \times \int_{x_h}^1 \frac{dx}{x} f_{a/N}(x) \hat{H}_{ia \rightarrow j}(\xi, \zeta, x; k') + \dots \quad (8)$$

where i, j, a include all QED and QCD particles. The lower limits z_L, x_L and x_h depend on external kinematics, and the ellipsis represents $1/\ell_T^2$ corrections. In Eq. (8), the LDF $f_{i/e}(\xi)$ gives the probability to find lepton i with light-cone momentum $\xi\ell^+$ in the incident lepton e , while the LFF $D_{e/j}(\zeta)$ describes the emergence of the final lepton e . The LDF and LFF are defined in analogy with the quark PDF in the nucleon, $f_{a/N}(x)$, where $x = p^+/P^+$ is the nucleon momentum fraction carried by the quark, and quark to hadron fragmentation function [167], with the quark and gluon fields replaced by lepton and photon fields, and the hadron state by a lepton state.

In Eq. (8), the $\hat{H}_{ia \rightarrow j}$ is lepton-parton scattering cross section with all logarithmic CO sensitivities along the direction of observed momenta, ℓ, ℓ' and P , removed, and is therefore IR safe and insensitive to taking $m_e \rightarrow 0$. The IR-safe $\hat{H}_{ia \rightarrow j}$ can be perturbatively calculated by expanding the factorized formula (8) order-by-order in powers of α and α_s , with $\hat{H}_{ia \rightarrow j}^{(m,n)}$ denoting the contribution at $\mathcal{O}(\alpha^m \alpha_s^n)$. The factorized inclusive DIS cross section in Eq. (8) resums large photon radiation collinearly sensitive to the incident lepton into $f_{i/e}$, and radiation that is collinearly sensitive to the scattered lepton into $D_{e/j}$, and takes care of the photon radiation collinear to the colliding nucleon by adding QED corrections to the evolution kernels of the nucleon PDF $f_{a/N}$.

QED contributions— As for the factorized QCD case, the QED contribution to inclusive eN scattering is organized into CO sensitive LDFs and LFFs, and IR-safe hard scattering functions. Unlike the PDFs in QCD, however, which are nonperturbative, LDFs and LFFs are calculable perturbatively in QED. Focusing for brevity only on the “valence” lepton part [$i = j = e$ in Eq. (8)], at

leading order (LO) in α we have $f_{e/e}^{(0)}(\xi) = \delta(\xi - 1)$, and similarly the LFFs at LO are given by $D_{e/e}^{(0)}(\zeta) = \delta(\zeta - 1)$. Explicit expressions for $f_{e/e}^{(1)}(\xi)$ and $D_{e/e}^{(1)}(\zeta)$ are given in Ref. [154]. Expanding to lowest order [$\mathcal{O}(\alpha^2\alpha_s^0)$], we have

$$E' \frac{d\sigma_{\text{DIS}}}{d^3\ell'} \approx \frac{2\alpha^2}{s} \sum_q \int_{z_L}^1 \frac{d\zeta}{\zeta^2} \int_{x_L}^1 \frac{d\xi}{\xi} D_{e/e}(\zeta) f_{e/e}(\xi) \times \int_{x_h}^1 \frac{dx}{x} e_q^2 f_{q/N}(x) \frac{x^2 \zeta [(\xi \zeta s)^2 + u^2]}{(\xi t)^2 (\xi \zeta s + u)} \delta(x - x_h). \quad (9)$$

With the factorization formalism in Eq. (8), one can systematically improve the ‘‘RCs’’ by calculating the IR-safe hard parts $\widehat{H}_{e \rightarrow e}^{(m,n)}$ perturbatively for $m > 2$, and determining the universal, LDFs and LFFs.

Numerical impact— In general, the larger the momentum transfer Q^2 , or more available phase space $s \gg Q^2$, the more important are the RCs. In our factorization approach, the logarithmically enhanced RCs are included in the universal LDFs and LFFs, which shift the momenta of active leptons, and consequently impact the momentum transfer to the colliding nucleon. To demonstrate the numerical impact of RCs, we show in Fig. 14 the ratio of the DIS cross sections $\sigma \equiv E' d\sigma_{\text{DIS}}/d^3\ell'$ without RCs (‘‘ $\sigma_{\text{no RC}}$ ’’) and including RCs (‘‘ σ_{RC} ’’), where $\sigma_{\text{no RC}}$ is given by Eq. (9) with $f_{e/e} \rightarrow f_{e/e}^{(0)}$ and $D_{e/e} \rightarrow D_{e/e}^{(0)}$. The cross section σ_{RC} is also given by Eq. (9) but evaluated with (i) NLO: $f_{e/e} = f_{e/e}^{(0)} + f_{e/e}^{(1)}$ and $D_{e/e} = D_{e/e}^{(0)} + D_{e/e}^{(1)}$, (ii) RES_I: resummed (or evolved) LDF and LFF with input distribution $f_{e/e} = f_{e/e}^{(0)}$ and $D_{e/e} = D_{e/e}^{(0)}$ at $\mu_0^2 = m_e^2$, or (iii) RES_{II}: resummed LDF and LFF with input $f_{e/e} = f_{e/e}^{(0)} + f_{e/e}^{(1)}$ and $D_{e/e} = D_{e/e}^{(0)} + D_{e/e}^{(1)}$.

The results in Fig. 14, shown for kinematics typical of Jefferson Lab experiments and those planned for the EIC, illustrate some surprising and rather dramatic effects of RCs in certain regions of phase space. Defining $y_{\ell'}$ to be the scattered lepton rapidity, the ratio $\sigma_{\text{no RC}}/\sigma_{\text{RC}}$ versus ℓ'_T was shown for several fixed values of $y_{\ell'}$ typical for JLab [Fig. 14(a)] and EIC [Fig. 14(b)] kinematics. The general trend of the effects is an increase in the magnitude of the correction at lower ℓ'_T , consistent with more phase space available for photon radiation. With the greater phase space available at the EIC, the RC effects can become quite significant at lower ℓ'_T values, even with $\ell'_T > 1$ GeV, and the differences between the RC prescriptions (NLO, RES_I or RES_{II}) become more evident. While the differences between the NLO and resummed results can be large, the differences between the two resummed versions, RES_I and RES_{II}, are much smaller. This suggests that the resummation effects are important and the uncertainty in choosing the input distributions is mild, which provides greater stability in our factorization approach to calculate QED contribution to inelastic lepton-hadron scattering.

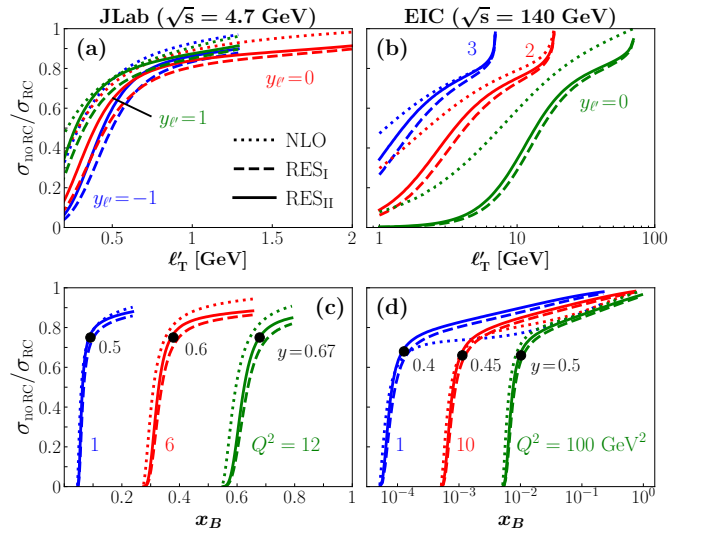


FIG. 14. Ratios of inclusive ep cross sections with no RCs to those including RCs computed according to the NLO (dotted lines), RES_I (dashed lines), and RES_{II} (solid lines) schemes, referred to in the text [154]. The values of y at which the RCs are $\gtrsim 30\%$ are marked by the black filled circles.

The impact of the RCs can be more directly visualized in terms of the traditional DIS variables x_B and Q^2 , and in Fig. 14(c)–(d) the ratio $\sigma_{\text{no RC}}/\sigma_{\text{RC}}$ is shown versus x_B at fixed Q^2 . The most striking feature for both JLab and EIC kinematics is the dramatic change of slope in the x_B dependence, from relatively shallow at higher x_B , where the RCs are $\lesssim 20\%$, to a steep fall-off with decreasing x_B . For JLab kinematics this turnover occurs when $y \approx 0.5 - 0.6$, depending on the Q^2 value, but at even smaller values, $y \approx 0.4$, for EIC kinematics. Our results in Fig. 14 clearly indicate that extreme care should be taken when extracting partonic information from inclusive DIS data at low x_B and high Q^2 , in view of the potentially large uncertainties in the QED RCs.

Outlook— Our unified factorization approach to QED and QCD dynamics has important implications for future analyses of hard scattering at the EIC. Our observation that, without being able to account for all radiation, the photon-hadron frame is not well-defined and the standard x_B and Q^2 does not fully control the momentum transfer to the colliding hadron, could impact the precision with which one can extract TMDs and explore the nucleon’s 3-dimensional landscape in momentum space. On the other hand, our unified factorization approach allows the systematic resummation of the logarithmically enhanced RCs into factorized LDFs and LFFs that are universal for all final states, leaving the fixed order QED corrections completely IR-safe and stable as $m_e \rightarrow 0$. In contrast to previous treatments of RCs computed for different observables, the new paradigm allows a uniform treatment of QED RCs for the extraction of PDFs, TMDs and other partonic correlation functions from lepton-hadron collision data.

Radiative Corrections in MC for EIC

Andrea Bressan

In the one-photon exchange approximation, and taking into account the transverse momentum of the produced hadron \vec{P}_{hT} the SIDIS cross-section is differential in five independent variables $\frac{d^5\sigma}{dx dy dz dP_{hT}^2 d\phi_h} (\equiv d^5\sigma)$ [86, 168]; in the unpolarized case, were we don't take into account neither the lepton nor the proton polarization we may write:

$$d^5\sigma = \frac{\alpha^2}{xyQ^2} \left[(1-y) + \frac{y^2}{2} \right] F_2(x, Q^2) \times \quad (10)$$

$$\left. \begin{aligned} & M_{UU}^h(x, Q^2, z, P_{hT}^2) \{1 + \\ & \frac{2(2-y)\sqrt{1-y}}{1+(1-y)^2} A_{UU}^{\cos\phi_h}(x, Q^2, z, P_{hT}^2) \cos\phi_h + \\ & \frac{2(1-y)}{1+(1-y)^2} A_{UU}^{\cos 2\phi_h}(x, Q^2, z, P_{hT}^2) \cos 2\phi_h \} \end{aligned} \right\}$$

with the amplitudes of the $\cos\phi_h$ and $\cos 2\phi_h$ ($A_{UU}^{\cos\phi_h}$ and $A_{UU}^{\cos 2\phi_h}$) modulations that are the ratio of semi-inclusive and inclusive form factors:

$$A_{UU}^{\cos X\phi_h} = \frac{F_{UU}^{\cos X\phi_h}}{F_2} \quad (11)$$

As can be seen from Fig. 15, we indicate the magnitude of the transverse momentum of the hadron h with respect of the virtual photon γ^* with P_{hT} , and with ϕ_h the azimuthal angle of the hadron- γ^* plane with respect to the lepton ℓ - ℓ' plane. Finally z is the fraction of the virtual photon energy taken by the hadron h .

From the cross section in Eq. 11 is therefore evident the importance of a correct evaluation of the direction of the virtual photon. All the azimuthal modulations (including the single spin asymmetries for the polarized case) are evaluated starting from this direction; and the same happens for the P_{hT} -dependent quantities, such as the P_{hT} -dependent multiplicities, indicated with M_{UU}^h in Eq. 11.

Photon radiation from the lepton lines changes the DIS kinematics on the event-by-event basis. The true virtual photon direction and momentum are different than the

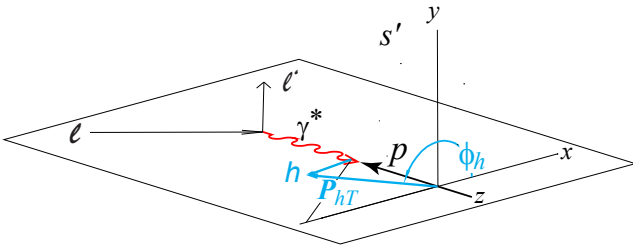


FIG. 15. DIS scattering with hadron production in the Gamma Nucleon System

one reconstructed from the leptons. This introduces false asymmetries in the azimuthal distribution of hadrons as calculated with respect to the reconstructed hadron- γ^* plane and smears the the kinematic distributions of z and P_{hT} . Due to the energy unbalance, the reconstructed energy of the γ^* is always larger than the true one independently of if the photon was radiated by the incoming or by the outgoing lepton, in the same way as the polar angle of the virtual photon with respect of the incoming muon in the Laboratory System is always larger for the reconstructed γ^* (as an example see in Fig. 16 the results for scattering of 5 GeV electrons on 50 GeV).

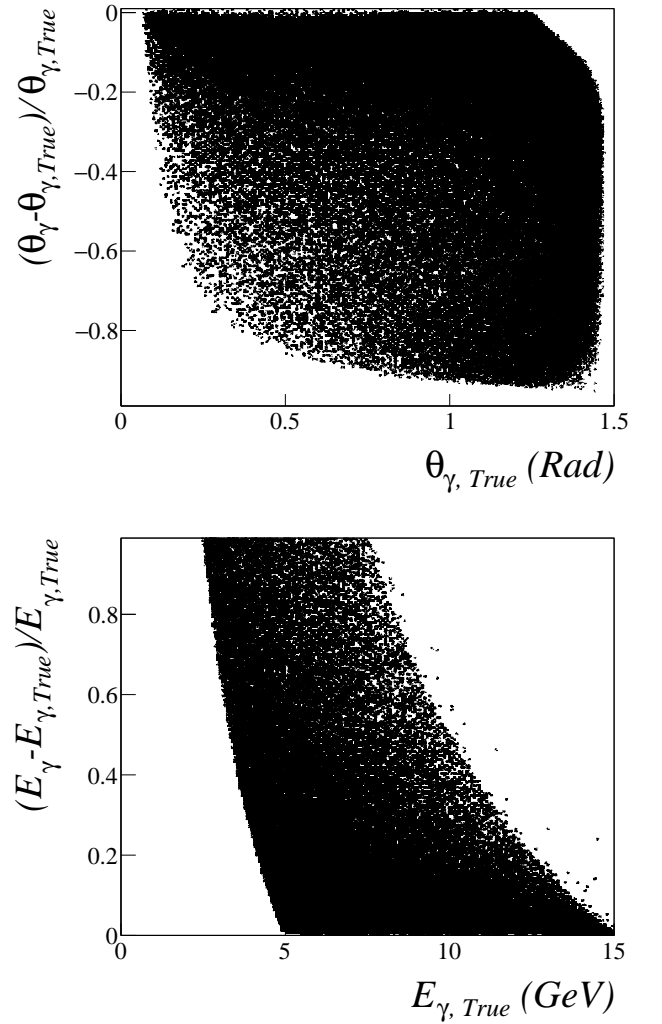


FIG. 16. Relative difference between the polar θ_γ angle of the virtual photon with respect to the incoming lepton beam in the Laboratory system protons as a function of θ_γ in the Lab for the scattering of 5 GeV electrons on 50 GeV (left). Same for the virtual photon energy but in the GNS (right).

The bias in the reconstructed virtual photon direction introduce quite sizable azimuthal modulations modulations, which impact on TMDs entering the unpolarized cross section. Since also the experimental apparatus may show some modulation in the acceptance, it is important

to fold together a Monte Carlo encoding radiative effects in full simulations to calculate this experimental acceptance since these modulations will mix together in the real data.

Opportunities at EIC with Both Lepton Signs

Richard Milner

Radiative corrections have been calculated predominantly in a single photon approximation with simple estimation of multi-photon contributions until the beginning of this century, when a large discrepancy was observed between cross section and recoil polarization determinations in the GeV region of the ratio of the proton's elastic form factors. The widely accepted explanation is that hard two-photon effects have been neglected and affect the cross section determination. Measurements of the positron to electron cross section ratio have been carried out at DESY, Jefferson Lab and VEPP-2 up to Q^2 of about 2.4 (GeV/c)^2 but the results are inconclusive - see Axel's contribution here. Further measurements to higher Q^2 , where the contribution to the ratio should be larger, are under consideration at DESY by the TPEX collaboration and at Jefferson Lab, if a positron source can be realized.

Given that multi-photon effects are accepted to be essential in understanding GeV elastic electron-proton scattering, the fundamental process in hadron structure, it is certainly possible that these will also be significant for the new processes planned for study at EIC.

In addition, there are strong arguments to motivate the capability to have EIC positron beams based on compelling, open questions in hadron structure. Here, the charged current (CC) interaction, shown in Fig. 17, mediated by exchange of W^+ (W^-), becomes accessible by hard scattering of a positron (electron) from the hadronic target where the final-state lepton is a (undetectable) neutrino. Highlights include:

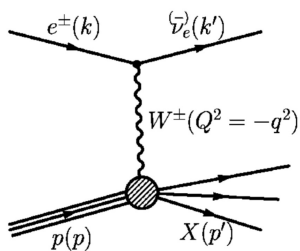


FIG. 17. Feynman diagram for the charge current electroweak interaction.

- Flavor separation
Using the CC electroweak interaction, it is possible to probe the d/u ratio at large x , the light quark sea asymmetry and the strange/antistrange quark parton distribution functions.
- Electroweak structure functions
Using spin-dependent CC scattering, new structure functions, arising from W^\pm exchange, can be

accessed that involve *charmed*, *strange* as well as *up* and *down* quarks. Further, as with the Bjorken Sum Rule for *up* and *down* quarks, there are also fundamental sum rules for these new structure functions. Experimental measurement of these sum rules can test our understanding of QCD.

- Deeply Virtual Compton Scattering(DVCS)
The DVCS process is the leading deeply virtual exclusive process for pursuing new insights into hadron structure with EIC. It will allow access to new Generalized Parton Distributions and has the potential to give insight into the origin of nucleon spin, if Ji's sum rule can be determined. In particular, measurement of the beam charge asymmetry for DVCS (pioneered by the HERMES experiment) uniquely allows access to the real part of the Bethe-Heitler-DVCS interference term.

In summary, as changing the lepton sign is key to experimentally accessing multi-photon contributions, measurement of the CC electroweak process and the full exploration of the DVCS process, it seems prudent to build the capability to have positron as well as electron beams into the next-generation, billion \$-class electron scattering facility.

-
- [1] F. Bloch and A. Nordsieck, Note on the radiation field of the electron, *Phys. Rev.* **52**, 54 (1937).
- [2] L. W. Mo and Y.-S. Tsai, Radiative Corrections to Elastic and Inelastic $e p$ and μp Scattering, *Rev.Mod.Phys.* **41**, 205 (1969).
- [3] D. R. Yennie, S. C. Frautschi, and H. Suura, The infrared divergence phenomena and high-energy processes, *Annals Phys.* **13**, 379 (1961).
- [4] G. Passarino, A practical approach for exponentiation of qcd corrections in arbitrary processes, *Nuclear Physics B* **619**, 313–358 (2001).
- [5] J. M. Friedrich, *Messung der virtuellen Comptonstreuung an MAMI zur Bestimmung generalisierter Polarisiertbarkeiten des Protons [in German]*, Ph.D. thesis, Mainz (2000).
- [6] A. V. Gramolin, V. S. Fadin, A. L. Feldman, R. E. Gerasimov, D. M. Nikolenko, I. A. Rachek, and D. K. Toporkov, A new event generator for the elastic scattering of charged leptons on protons, *J. Phys.* **G41**, 115001 (2014), [arXiv:nucl-ex/1401.2959 \[nucl-ex\]](#).
- [7] B. e. a. Adams, *COMPASS++/AMBER: Proposal for Measurements at the M2 beam line of the CERN SPS Phase-1: 2022-2024*, Tech. Rep. CERN-SPSC-2019-022. SPSC-P-360 (CERN, Geneva, 2019) the collaboration has not yet constituted itself, thus instead of a Spokesperson currently the nominated Contact Person is acting in place.
- [8] B. Henderson *et al.* (OLYMPUS), Hard Two-Photon Contribution to Elastic Lepton-Proton Scattering: Determined by the OLYMPUS Experiment, *Phys. Rev. Lett.* **118**, 092501 (2017), [arXiv:1611.04685 \[nucl-ex\]](#).
- [9] A. A. *et al.*, Electron ion collider: The next qcd frontier - understanding the glue that binds us all (2014), [arXiv:1212.1701 \[nucl-ex\]](#).
- [10] R. C. Walker *et al.*, Measurements of the proton elastic form factors for $1 \leq Q^2 \leq 3$ (GeV/c)² at SLAC, *Phys. Rev. D* **49**, 5671 (1994).
- [11] L. Andivahis *et al.*, Measurements of the electric and magnetic form-factors of the proton from $Q^2 = 1.75$ to 8.83 (GeV/c)², *Phys. Rev. D* **50**, 5491 (1994).
- [12] I. A. Qattan *et al.*, Precision rosenbluth measurement of the proton elastic form factors, *Phys. Rev. Lett.* **94**, 142301 (2005).
- [13] M. K. Jones *et al.*, G_E^p/G_M^p Ratio by Polarization Transfer in $\bar{e}p \rightarrow e\bar{p}$, *Phys. Rev. Lett.* **84**, 1398 (2000).
- [14] O. Gayou *et al.*, Measurement of G_E^p/G_M^p in $\bar{e}p \rightarrow e\bar{p}$ to $Q^2 = 5.6$ GeV², *Phys. Rev. Lett.* **88**, 092301 (2002).
- [15] V. Punjabi *et al.*, Proton elastic form factor ratios to $Q^2 = 3.5$ GeV² by polarization transfer, *Phys. Rev. C* **71**, 055202 (2005).
- [16] A. J. R. Puckett *et al.*, Recoil polarization measurements of the proton electromagnetic form factor ratio to $Q^2 = 8.5$ GeV², *Phys. Rev. Lett.* **104**, 242301 (2010).
- [17] A. J. R. Puckett *et al.*, Final analysis of proton form factor ratio data at $Q^2 = 4.0, 4.8,$ and 5.6 GeV², *Phys. Rev. C* **85**, 045203 (2012).
- [18] P. G. Blunden, W. Melnitchouk, and J. A. Tjon, Two-photon exchange and elastic electron-proton scattering, *Phys. Rev. Lett.* **91**, 142304 (2003).
- [19] P. A. M. Guichon and M. Vanderhaeghen, How to reconcile the rosenbluth and the polarization transfer methods in the measurement of the proton form factors, *Phys. Rev. Lett.* **91**, 142303 (2003).
- [20] J. Ahmed, P. G. Blunden, and W. Melnitchouk, Two-photon exchange form intermediate state resonances in elastic electron-proton scattering, *Phys. Rev. C* **102**, 045205 (2020).
- [21] P. G. Blunden and W. Melnitchouk, Dispersive approach to two-photon exchange in elastic electron-proton scattering, *Phys. Rev. C* **95**, 065209 (2017).
- [22] M. Tanabashi *et al.*, Review of particle physics, *Phys. Rev. D* **98**, 030001 (2018).
- [23] V. I. Mokeev *et al.*, Experimental study of the $P_{11}(1440)$ and $D_{13}(1520)$ resonances from the CLAS data on $ep \rightarrow e'\pi^+\pi^-p'$, *Phys. Rev. C* **86**, 035203 (2012).
- [24] A. N. Hiller Blin *et al.*, Nucleon resonance contributions to unpolarized inclusive electron scattering, *Phys. Rev. C* **100**, 035201 (2019).
- [25] I. G. Aznauryan and V. D. Burkert, Electroexcitation of nucleon resonances, *Prog. Part. Nucl. Phys.* **67**, 1 (2012).
- [26] J. J. Kelly, Simple parametrization of nucleon form factors, *Phys. Rev. C* **70**, 068202 (2004).
- [27] D. Rimal *et al.*, Measurement of two-photon exchange effect by comparing elastic $e^\pm p$ cross sections, *Phys. Rev. C* **95**, 065201 (2017).
- [28] I. A. Rachek *et al.*, Measurement of the two-photon exchange contribution to the elastic $e^\pm p$ scattering cross sections at the VEPP-3 storage ring, *Phys. Rev. Lett.* **114**, 062005 (2015).
- [29] B. S. Henderson *et al.*, Hard two-photon contribution to elastic lepton-proton scattering determined by the OLYMPUS experiment, *Phys. Rev. Lett.* **118**, 092501 (2017).
- [30] A. V. Gramolin and D. M. Nikolenko, Reanalysis of Rosenbluth measurements of the proton form factors, *Phys. Rev. C* **93**, 055201 (2016), [arXiv:1603.06920 \[nucl-ex\]](#).
- [31] A. Afanasev, I. Akushevich, A. Ilyichev, and B. Nizyoporuk, ELRADGEN: Monte Carlo generator for radiative events in elastic electron proton scattering, *Czech. J. Phys.* **53**, B449 (2003), [arXiv:hep-ph/0308106](#).
- [32] O. Koshchii and A. Afanasev, Charge asymmetry in elastic scattering of massive leptons on protons, *Phys. Rev. D* **96**, 016005 (2017).
- [33] O. Koshchii and A. Afanasev, Contribution of σ meson exchange to elastic lepton-proton scattering, *Phys. Rev. D* **94**, 116007 (2016).
- [34] O. Koshchii and A. Afanasev, Lepton mass effects for beam-normal single-spin asymmetry in elastic muon-proton scattering, *Phys. Rev. D* **100**, 096020 (2019).
- [35] O. Tomalak and M. Vanderhaeghen, Two-photon exchange corrections in elastic muon-proton scattering, *Phys. Rev. D* **90**, 013006 (2014).
- [36] A. Afanasev and A. Ilyichev, Contribution of hard photon emission to charge asymmetry in elastic (anti)lepton-proton scattering (2020) [arXiv:2007.02087 \[hep-ph\]](#).
- [37] R. Gilman *et al.* (MUSE), Technical Design Report for the Paul Scherrer Institute Experiment R-12-01.1: Studying the Proton "Radius" Puzzle with μp Elastic Scattering, (2017), [arXiv:1709.09753 \[physics.ins-det\]](#).
- [38] L. C. Maximon and J. A. Tjon, Radiative corrections to electron-proton scattering, *Phys. Rev. C* **62**, 054320 (2000), [arXiv:0002058 \[nucl-th\]](#).

- [39] I. Akushevich, O. Filoti, A. Ilyichev, and N. Shumeiko, Monte Carlo Generator ELRADGEN 2.0 for Simulation of Radiative events in Elastic ep-Scattering of Polarized Particles, *Comput. Phys. Commun.* **183**, 1448 (2012), [arXiv:1104.0039 \[hep-ph\]](#).
- [40] J. C. Bernauer, *Measurement of the elastic electron-proton cross section and separation of the electric and magnetic form factor in the Q^2 range from 0.004 to 1 (GeV/c)²*, Ph.D. thesis, Johannes Gutenberg-Universität Mainz, Mainz, Germany (2010).
- [41] P. Talukdar, F. Myhrer, G. Meher, and U. Raha, Low-Energy Lepton-Proton Bremsstrahlung via Effective Field Theory, *Eur. Phys. J. A* **54**, 195 (2018), [arXiv:1810.04027 \[nucl-th\]](#).
- [42] I. A. Rachek *et al.*, Measurement of the two-photon exchange contribution to the elastic $e^\pm p$ scattering cross sections at the VEPP-3 storage ring, *Phys. Rev. Lett.* **114**, 062005 (2015), [arXiv:1411.7372 \[nucl-ex\]](#).
- [43] D. Adikaram *et al.* (CLAS), Towards a resolution of the proton form factor problem: new electron and positron scattering data, *Phys. Rev. Lett.* **114**, 062003 (2015), [arXiv:1411.6908 \[nucl-ex\]](#).
- [44] P. G. Blunden and W. Melnitchouk, Dispersive approach to two-photon exchange in elastic electron-proton scattering, *Phys. Rev.* **C95**, 065209 (2017), [arXiv:1703.06181 \[nucl-th\]](#).
- [45] J. Bernauer *et al.* (A1), Electric and magnetic form factors of the proton, *Phys. Rev.* **C90**, 015206 (2014).
- [46] A. Schmidt, How much two-photon exchange is needed to resolve the proton form factor discrepancy?, *J. Phys. G* **47**, 055109 (2020), [arXiv:1907.07318 \[nucl-ex\]](#).
- [47] A. V. Afanasev, S. J. Brodsky, C. E. Carlson, Y.-C. Chen, and M. Vanderhaeghen, The Two-photon exchange contribution to elastic electron-nucleon scattering at large momentum transfer, *Phys. Rev.* **D72**, 013008 (2005), [arXiv:0502013 \[hep-ph\]](#).
- [48] N. Kivel and M. Vanderhaeghen, Two-photon exchange in elastic electron-proton scattering: QCD factorization approach, *Phys. Rev. Lett.* **103**, 092004 (2009), [arXiv:0905.0282 \[hep-ph\]](#).
- [49] A. Afanasev, P. G. Blunden, D. Hasell, and B. A. Raue, Two-photon exchange in elastic electron-proton scattering, *Prog. Part. Nucl. Phys.* **95**, 245 (2017), [arXiv:1703.03874 \[nucl-ex\]](#).
- [50] A. Schmidt, *Measuring the lepton sign asymmetry in elastic electron-proton scattering with OLYMPUS*, Ph.D. thesis, MIT (2016), [arXiv:1711.09894 \[nucl-ex\]](#).
- [51] J. Bernauer *et al.*, OLYMPUS: First measurement of the charge-averaged elastic lepton-proton scattering cross section, (2020), [arXiv:2008.05349 \[nucl-ex\]](#).
- [52] A. Accardi *et al.*, e^+ @JLab White Paper: An Experimental Program with Positron Beams at Jefferson Lab, (2020), [arXiv:2007.15081 \[nucl-ex\]](#).
- [53] W. Xiong *et al.*, A small proton charge radius from an electron-proton scattering experiment, *Nature* **575**, 147 (2019).
- [54] W. Xiong, “A High Precision Measurement of the Proton Charge Radius at JLab”, PhD Thesis, Department of Physics, Duke University (2020).
- [55] I. Akushevich, H. Gao, A. Ilyichev, and M. Meziane, Radiative corrections beyond the ultra relativistic limit in unpolarized ep elastic and Møller scatterings for the PRad Experiment at Jefferson Laboratory, *Eur. Phys. J. A* **51**, 1 (2015).
- [56] D. Bardin and N. Shumeiko, An Exact Calculation of the Lowest Order Electromagnetic Correction to the Elastic Scattering, *Nucl. Phys. B* **127**, 242 (1977).
- [57] C. Peng, “PRadAnalyzerPackage”, Department of Physics, Duke University (2017), <https://github.com/JeffersonLab/PRadAnalyzer>.
- [58] A. Arbuzov and T. Kopylova, On higher order radiative corrections to elastic electron-proton scattering, *Eur. Phys. J. C* **75**, 603 (2015), [arXiv:1510.06497 \[hep-ph\]](#).
- [59] A. Aleksejevs, S. Barkanova, V. Zykunov, and E. Kuraev, Estimating two-loop radiative effects in the MOLLER experiment, *Phys. Atom. Nucl.* **76**, 888 (2013).
- [60] A. Gasparian, H. Gao, D. Dutta, N. Liyanage, E. Pasyuk, D. Higinbotham, C. Peng, K. Gnanvo, W. Xiong, and X. Bai (PRad), “PRad-II: A New Upgraded High Precision Measurement of the Proton Charge Radius” (2020), [arXiv:2009.10510 \[nucl-ex\]](#).
- [61] S. Srednyak, I. Akushevich, and A. Ilyichev, Private communication, (2020).
- [62] PRad Collaboration, “Precision Deuteron Charge Radius Measurement with Elastic Electron-Deuteron Scattering”, https://www.jlab.org/exp_prog/proposals/17/PR12-17-009.pdf.
- [63] I. Akushevich and N. Shumeiko, Radiative effects in deep inelastic scattering of polarized leptons by polarized light nuclei, *J. Phys. G* **20**, 513 (1994).
- [64] I. Akushevich, A. Ilyichev, and N. Shumeiko, Radiative effects in scattering of polarized leptons by polarized nucleons and light nuclei, in *20th International Symposium on Lepton and Photon Interactions at High Energies (LP 01)* (2001) [arXiv:hep-ph/0106180](#).
- [65] C. Gu, “e+d event generator”, Department of Physics, Duke University (2017).
- [66] J. Dudek *et al.*, Physics Opportunities with the 12 GeV Upgrade at Jefferson Lab, *Eur. Phys. J. A* **48**, 187 (2012), [arXiv:1208.1244 \[hep-ex\]](#).
- [67] J. Chen, H. Gao, T. Hemmick, Z. E. Meziani, and P. Souder (SoLID), “A White Paper on SoLID (Solenoidal Large Intensity Device)” (2014), [arXiv:1409.7741 \[nucl-ex\]](#).
- [68] I. Akushevich and A. Ilyichev, Lowest order QED radiative effects in polarized SIDIS, *Phys. Rev. D* **100**, 033005 (2019), [arXiv:1905.09232 \[hep-ph\]](#).
- [69] L. Guilhoto, “Applying Markov Chains to Monte Carlo Integration”, <http://math.uchicago.edu/~may/REU2017/REUPapers/Guilhoto.pdf>.
- [70] R. Pohl, R. Gilman, G. A. Miller, and K. Pachucki, Muonic hydrogen and the proton radius puzzle, *Annual Review of Nuclear and Particle Science* **63**, 175 (2013).
- [71] J. Bernauer *et al.* (A1), High-precision determination of the electric and magnetic form factors of the proton, *Phys. Rev. Lett.* **105**, 242001 (2010), [arXiv:1007.5076 \[nucl-ex\]](#).
- [72] M. Mihovilović *et al.*, First measurement of proton’s charge form factor at very low Q^2 with initial state radiation, *Phys. Lett. B* **771**, 194 (2017), [arXiv:1612.06707 \[nucl-ex\]](#).
- [73] R. Gilman *et al.* (MUSE), Studying the Proton “Radius” Puzzle with μp Elastic Scattering, (2013), [arXiv:1303.2160 \[nucl-ex\]](#).
- [74] P. Talukdar, S. V.C., U. Raha, and F. Myhrer, Radiative corrections to elastic lepton-proton scattering at next-to-leading order in chiral perturbation theory, preprint

in preparation.

- [75] V. Bernard, N. Kaiser, and U.-G. Meissner, Chiral dynamics in nucleons and nuclei, *Int. J. Mod. Phys. E* **4**, 193 (1995), [arXiv:hep-ph/9501384](#).
- [76] P. Talukdar, V. C. Shastry, U. Raha, and F. Myhrer, Lepton-Proton Two-Photon Exchange in Chiral Perturbation Theory, *Phys. Rev. D* **101**, 013008 (2020), [arXiv:1911.06843 \[nucl-th\]](#).
- [77] M. Vanderhaeghen, J. Friedrich, D. Lhuillier, D. Marchand, L. Van Hoorebeke, and J. Van de Wiele, QED radiative corrections to virtual Compton scattering, *Phys. Rev. C* **62**, 025501 (2000), [arXiv:hep-ph/0001100](#).
- [78] I. Akushevich, H. Bottcher, and D. Ryckbosch, Radgen 1.0: Monte carlo generator for radiative events in dis on polarized and unpolarized targets, in *Workshop on Monte Carlo Generators for HERA Physics (Plenary Starting Meeting)* (1998) pp. 554–565, [hep-ph/9906408](#).
- [79] T. Sjostrand, S. Mrenna, and P. Z. Skands, PYTHIA 6.4 Physics and Manual, *JHEP* **0605**, 026, [arXiv:hep-ph/0603175 \[hep-ph\]](#).
- [80] G. Ingelman, A. Edin, and J. Rathsman, LEPTO 6.5: A Monte Carlo generator for deep inelastic lepton - nucleon scattering, *Comput.Phys.Commun.* **101**, 108 (1997), [arXiv:hep-ph/9605286 \[hep-ph\]](#).
- [81] L. Mankiewicz, A. Schafer, and M. Veltri, Peps: A monte carlo generator for polarized leptoproduction, *Comput. Phys. Commun.* **71**, 305 (1992).
- [82] A. Kotzinian, New quark distributions and semiinclusive electroproduction on the polarized nucleons, *Nucl. Phys. B* **441**, 234 (1995), [hep-ph/9412283](#).
- [83] I. Akushevich, A. Ilyichev, N. Shumeiko, A. Soroko, and A. Tolkachev, POLRAD 2.0: FORTRAN code for the radiative corrections calculation to deep inelastic scattering of polarized particles, *Comput. Phys. Commun.* **104**, 201 (1997), [arXiv:hep-ph/9706516](#).
- [84] I. Akushevich, A. Ilyichev, and M. Osipenko, Complete lowest order radiative corrections to five-fold differential cross-section of hadron leptoproduction, *Phys.Lett. B* **672**, 35 (2009), [arXiv:0711.4789 \[hep-ph\]](#).
- [85] J. Levelt and P. Mulders, Quark correlation functions in deep inelastic semiinclusive processes, *Phys. Rev. D* **49**, 96 (1994), [arXiv:hep-ph/9304232](#).
- [86] A. Bacchetta *et al.*, Semi-inclusive deep inelastic scattering at small transverse momentum, *JHEP* **02**, 093, [arXiv:hep-ph/0611265](#).
- [87] D. Y. Bardin and N. Shumeiko, On an exact calculation of the lowest-order electromagnetic correction to the point particle elastic scattering, *Nuclear Physics B* **127**, 242 (1977).
- [88] A. Beyer *et al.*, The Rydberg constant and proton size from atomic hydrogen, *Science* **358**, 79 (2017).
- [89] N. Bezginov, T. Valdez, M. Horbatsch, A. Marsman, A. Vutha, and E. Hessels, A measurement of the atomic hydrogen Lamb shift and the proton charge radius, *Science* **365**, 1007 (2019).
- [90] R. Pohl *et al.*, The size of the proton, *Nature* **466**, 213 (2010).
- [91] A. Antognini *et al.*, Proton Structure from the Measurement of $2S - 2P$ Transition Frequencies of Muonic Hydrogen, *Science* **339**, 417 (2013).
- [92] B. de Beauvoir, F. Nez, L. Julien, B. Cagnac, F. Biraben, D. Touahri, L. Hilico, O. Acef, A. Clairon, and J. Zondy, Absolute Frequency Measurement of the S-2- S-8/D Transitions in Hydrogen and Deuterium: New Determination of the Rydberg Constant, *Phys. Rev. Lett.* **78**, 440 (1997).
- [93] C. Schwob, L. Jozefowski, B. de Beauvoir, L. Hilico, F. Nez, L. Julien, F. Biraben, O. Acef, J.-J. Zondy, and A. Clairon, Optical Frequency Measurement of the S-2-D-12 Transitions in Hydrogen and Deuterium: Rydberg Constant and Lamb Shift Determinations, *Phys. Rev. Lett.* **82**, 4960 (1999).
- [94] H. Fleurbaey, S. Galtier, S. Thomas, M. Bonnaud, L. Julien, F. Biraben, F. Nez, M. Abgrall, and J. Guéna, New Measurement of the $1S - 3S$ Transition Frequency of Hydrogen: Contribution to the Proton Charge Radius Puzzle, *Phys. Rev. Lett.* **120**, 183001 (2018), [arXiv:1801.08816 \[physics.atom-ph\]](#).
- [95] A. J. Krasznahorkay *et al.*, Observation of Anomalous Internal Pair Creation in Be8 : A Possible Indication of a Light, Neutral Boson, *Phys. Rev. Lett.* **116**, 042501 (2016), [arXiv:1504.01527 \[nucl-ex\]](#).
- [96] A. Krasznahorkay *et al.*, On the creation of the 17 MeV X boson in the 17.6 MeV M1 transition of ^8Be , *EPJ Web Conf.* **142**, 01019 (2017).
- [97] A. Krasznahorkay *et al.*, New evidence supporting the existence of the hypothetical X17 particle, (2019), [arXiv:1910.10459 \[nucl-ex\]](#).
- [98] U. D. Jentschura and I. Nándori, Atomic Physics Constraints on the X Boson, *Phys. Rev. A* **97**, 042502 (2018), [arXiv:1804.03096 \[hep-ph\]](#).
- [99] U. D. Jentschura, Fifth Force and Hyperfine Splitting in Bound Systems, *Phys. Rev. A* **101**, 062503 (2020), [arXiv:2003.07207 \[hep-ph\]](#).
- [100] U. Ellwanger and S. Moretti, Possible Explanation of the Electron Positron Anomaly at 17 MeV in ^8Be Transitions Through a Light Pseudoscalar, *JHEP* **11**, 039, [arXiv:1609.01669 \[hep-ph\]](#).
- [101] J. L. Feng, B. Fornal, I. Galon, S. Gardner, J. Smolinsky, T. M. P. Tait, and P. Tanedo, Protophobic Fifth-Force Interpretation of the Observed Anomaly in ^8Be Nuclear Transitions, *Phys. Rev. Lett.* **117**, 071803 (2016), [arXiv:1604.07411 \[hep-ph\]](#).
- [102] J. L. Feng, B. Fornal, I. Galon, S. Gardner, J. Smolinsky, T. M. P. Tait, and P. Tanedo, Particle physics models for the 17 MeV anomaly in beryllium nuclear decays, *Phys. Rev. D* **95**, 035017 (2017), [arXiv:1608.03591 \[hep-ph\]](#).
- [103] C. Itzykson and J. Zuber, *Quantum Field Theory*, International Series In Pure and Applied Physics (McGraw-Hill, New York, 1980).
- [104] G. Soff, (1996), private communication.
- [105] U. Jentschura, G. Soff, V. Ivanov, and S. G. Karshenboim, The Bound $\mu^+ \mu^-$ system, *Phys. Rev. A* **56**, 4483 (1997), [arXiv:physics/9706026](#).
- [106] U. Jentschura, V. Ivanov, G. Soff, and S. G. Karshenboim, Next-to-leading and higher order corrections to the decay rate of dimuonium, *Phys. Lett. B* **424**, 397 (1998), [arXiv:hep-ph/9706401](#).
- [107] H. Lamm, Hadronic Vacuum Polarization in True Muonium, *Phys. Rev. A* **95**, 012505 (2017), [arXiv:1611.04258 \[physics.atom-ph\]](#).
- [108] L. Buonocore, P. Nason, F. Tramontano, and G. Zanderighi, Leptons in the proton, *JHEP* **08** (08), 019, [arXiv:2005.06477 \[hep-ph\]](#).
- [109] U. Jentschura, Light sea Fermions in electron-proton and muon-proton interactions, *Phys. Rev. A* **88**, 062514 (2013), [arXiv:1401.3666 \[physics.atom-ph\]](#).

- [110] L. Camilleri, J. Christenson, M. Kramer, L. Lederman, Y. Nagashima, and T. Yamanouchi, High-energy muon-proton scattering - muon-electron universality, *Phys. Rev. Lett.* **23**, 153 (1969).
- [111] G. A. Miller, Non-Perturbative Lepton Sea Fermions in the Nucleon and the Proton Radius Puzzle, *Phys. Rev. C* **91**, 055204 (2015), [arXiv:1501.01036 \[nucl-th\]](#).
- [112] U. Jentschura, Muonic bound systems, virtual particles and proton radius, *Phys. Rev. A* **92**, 012123 (2015), [arXiv:1411.4889 \[hep-ph\]](#).
- [113] R.-D. Bucoveanu and H. Spiesberger, Second-Order Leptonic Radiative Corrections for Lepton-Proton Scattering, *Eur. Phys. J. A* **55**, 57 (2019), [arXiv:1811.04970 \[hep-ph\]](#).
- [114] P. Banerjee, T. Engel, A. Signer, and Y. Ulrich, QED at NNLO with McMule, *SciPost Phys.* **9**, 027 (2020), [arXiv:2007.01654 \[hep-ph\]](#).
- [115] J. Kripfganz, H. Moring, and H. Spiesberger, Higher order leading logarithmic QED corrections to deep inelastic e p scattering at very high-energies, *Z. Phys. C* **49**, 501 (1991).
- [116] J. Blumlein and H. Kawamura, Universal higher order singlet QED corrections to unpolarized lepton scattering, *Eur. Phys. J. C* **51**, 317 (2007), [arXiv:hep-ph/0701019](#).
- [117] D. Becker *et al.*, The P2 experiment, *Eur. Phys. J. A* **54**, 208 (2018), [arXiv:1802.04759 \[nucl-ex\]](#).
- [118] W. Xiong, A. Gasparian, H. Gao, D. Dutta, M. Khandaker, N. Liyanage, E. Pasyuk, C. Peng, X. Bai, L. Ye, *et al.*, A small proton charge radius from an electron-proton scattering experiment, *Nature* **575**, 147 (2019).
- [119] R. Pohl, A. Antognini, F. Nez, F. D. Amaro, F. Biraben, J. M. Cardoso, D. S. Covita, A. Dax, S. Dhawan, L. M. Fernandes, *et al.*, The size of the proton, *nature* **466**, 213 (2010).
- [120] M. I. Eides, H. Grotch, and V. A. Shelyuto, Theory of light hydrogenlike atoms, *Physics Reports* **342**, 63 (2001).
- [121] A. Czarnecki, U. D. Jentschura, and K. Pachucki, Calculation of the one- and two-loop lamb shift for arbitrary excited hydrogenic states, *Physical review letters* **95**, 180404 (2005).
- [122] S. G. Karshenboim, Precision physics of simple atoms: QED tests, nuclear structure and fundamental constants, *Physics reports* **422**, 1 (2005).
- [123] J. Ahmed, P. Blunden, and W. Melnitchouk, Two-photon exchange from intermediate state resonances in elastic electron-proton scattering, (2020), [arXiv:2006.12543 \[nucl-th\]](#).
- [124] O. Tomalak and M. Vanderhaeghen, Dispersion relation formalism for the two-photon exchange correction to elastic muon-proton scattering: elastic intermediate state, *Eur. Phys. J. C* **78**, 514 (2018), [arXiv:1803.05349 \[hep-ph\]](#).
- [125] W. E. Caswell and G. P. Lepage, Effective lagrangians for bound state problems in qed, qcd, and other field theories, *Physics Letters B* **167**, 437 (1986).
- [126] S. Srednyak, Bound state equations in Riemannian geometry, (2018), [arXiv:1804.11306 \[hep-th\]](#).
- [127] I. V. Kanatchikov, Schrödinger Wave Functional in Quantum Yang-Mills Theory from Precanonical Quantization, *Rept. Math. Phys.* **82**, 373 (2018), [arXiv:1805.05279 \[hep-th\]](#).
- [128] C. Kiefer, Functional schrödinger equation for scalar qed, *Physical Review D* **45**, 2044 (1992).
- [129] S. J. Brodsky, H.-C. Pauli, and S. S. Pinsky, Quantum chromodynamics and other field theories on the light cone, *Physics Reports* **301**, 299 (1998).
- [130] K. Pachucki, Complete two-loop binding correction to the lamb shift, *Physical review letters* **72**, 3154 (1994).
- [131] R. Karplus, A. Klein, and J. Schwinger, Electrodynamic Displacement of Atomic Energy Levels. 2. Lamb Shift, *Phys. Rev.* **86**, 288 (1952).
- [132] R. Hotta and T. Tanisaki, *D-modules, perverse sheaves, and representation theory*, Vol. 236 (Springer Science & Business Media, 2007).
- [133] K. Takeuchi, Monodromy at infinity of a-hypergeometric functions and toric compactifications, *Mathematische Annalen* **348**, 815 (2010).
- [134] P. Banerjee *et al.*, Theory for muon-electron scattering @ 10 ppm: A report of the MUonE theory initiative, *Eur. Phys. J. C* **80**, 591 (2020), [arXiv:2004.13663 \[hep-ph\]](#).
- [135] S. Di Vita, T. Gehrmann, S. Laporta, P. Mastrolia, A. Primo, and U. Schubert, Master integrals for the NNLO virtual corrections to $q\bar{q} \rightarrow t\bar{t}$ scattering in QCD: the non-planar graphs, *JHEP* **06**, 117, [arXiv:1904.10964 \[hep-ph\]](#).
- [136] H. Frellesvig, F. Gasparotto, M. K. Mandal, P. Mastrolia, L. Mattiazzi, and S. Mizera, Vector Space of Feynman Integrals and Multivariate Intersection Numbers, *Phys. Rev. Lett.* **123**, 201602 (2019), [arXiv:1907.02000 \[hep-th\]](#).
- [137] I. Rachek *et al.*, Two-photon exchange contribution to elastic electron-proton scattering: measurements at the VEPP-3 storage ring, *Phys. Scripta T* **166**, 014017 (2015).
- [138] L. Adams, C. Bogner, and S. Weinzierl, The two-loop sunrise graph with arbitrary masses, *Journal of Mathematical Physics* **54**, 052303 (2013).
- [139] S. Bloch and P. Vanhove, The elliptic dilogarithm for the sunset graph, *Journal of Number Theory* **148**, 328 (2015).
- [140] S. Bloch, M. Kerr, and P. Vanhove, A feynman integral via higher normal functions, *Compositio Mathematica* **151**, 2329 (2015).
- [141] I. M. Gelfand, M. M. Kapranov, and A. V. Zelevinsky, Generalized euler integrals and a-hypergeometric functions, *Advances in Mathematics* **84**, 255 (1990).
- [142] S. Srednyak, Universal deformation of particle momenta space in perturbation theory, (2018), [arXiv:1805.00433 \[hep-th\]](#).
- [143] T. Oaku, Algorithms for the b-function and d-modules associated with a polynomial, *Journal of Pure and Applied Algebra* **117**, 495 (1997).
- [144] I. M. Gelfand, M. M. Kapranov, and A. V. Zelevinsky, A-discriminants, in *Discriminants, Resultants, and Multidimensional Determinants* (Springer, 1994) pp. 271–296.
- [145] V. Dolotin and A. Morozov, Introduction to nonlinear algebra. world sci., singapore, 2007, [arXiv preprint hep-th/0609022](#).
- [146] M. Spivakovsky, A solution to hironaka’s polyhedra game, in *Arithmetic and geometry* (Springer, 1983) pp. 419–432.
- [147] N. Hitchin *et al.*, Stable bundles and integrable systems, *Duke mathematical journal* **54**, 91 (1987).
- [148] W. Balsler, B. L. Braaksma, J.-P. Ramis, and Y. Sibuya,

- Multisummability of formal power series solutions of linear ordinary differential equations, *Asymptotic Analysis* **5**, 27 (1991).
- [149] C. Sabbah, *Introduction to Stokes structures*, Vol. 2060 (Springer, 2012).
- [150] T. Mochizuki, Wild harmonic bundles and wild pure twistor d -modules, arXiv preprint arXiv:0803.1344 (2008).
- [151] K. S. Kedlaya *et al.*, Good formal structures for flat meromorphic connections, i: surfaces, *Duke Mathematical Journal* **154**, 343 (2010).
- [152] C. Mitschi, D. Sauzin, M. Loday-Richaud, and É. Delabaere, *Divergent series, summability and resurgence* (Springer, 2016).
- [153] G. Ezra, K. Richter, G. Tanner, and D. Wintgen, Semi-classical cycle expansion for the helium atom, *Journal of Physics B: Atomic, Molecular and Optical Physics* **24**, L413 (1991).
- [154] T. Liu, W. Melnitchouk, J.-W. Qiu, and N. Sato, Factorized approach to radiative corrections for inelastic lepton-hadron collisions, (2020), arXiv:2008.02895 [hep-ph].
- [155] D. Bardin, C. Burdick, P. Khristova, and T. Riemann, Electroweak Radiative Corrections to Deep Inelastic Scattering at Hera. Neutral Current Scattering, *Z. Phys. C* **42**, 679 (1989).
- [156] R. Ent, B. Filippone, N. R. Makins, R. Milner, T. O'Neill, and D. Wasson, Radiative corrections for $(e, e\text{-prime } p)$ reactions at GeV energies, *Phys. Rev. C* **64**, 054610 (2001).
- [157] A. Afanasev, I. Akushevich, V. Burkert, and K. Joo, QED radiative corrections in processes of exclusive pion electroproduction, *Phys. Rev. D* **66**, 074004 (2002), arXiv:hep-ph/0208183.
- [158] J. C. Collins, D. E. Soper, and G. F. Sterman, Factorization of Hard Processes in QCD (1989) p. 1, arXiv:hep-ph/0409313.
- [159] S. Chekanov *et al.* (ZEUS), Measurement of the neutral current cross-section and $F(2)$ structure function for deep inelastic $e + p$ scattering at HERA, *Eur. Phys. J. C* **21**, 443 (2001), arXiv:hep-ex/0105090.
- [160] H. Abramowicz *et al.* (H1, ZEUS), Combination of measurements of inclusive deep inelastic $e^\pm p$ scattering cross sections and QCD analysis of HERA data, *Eur. Phys. J. C* **75**, 580 (2015), arXiv:1506.06042 [hep-ex].
- [161] A. Benvenuti *et al.* (BCDMS), A High Statistics Measurement of the Proton Structure Functions $F(2)(x, Q^2)$ and R from Deep Inelastic Muon Scattering at High Q^2 , *Phys. Lett. B* **223**, 485 (1989).
- [162] M. Adams *et al.* (E665), Proton and deuteron structure functions in muon scattering at 470-GeV, *Phys. Rev. D* **54**, 3006 (1996).
- [163] M. Arneodo *et al.* (New Muon), Measurement of the proton and deuteron structure functions, $F_2(p)$ and $F_2(d)$, and of the ratio $\sigma\text{-L} / \sigma\text{-T}$, *Nucl. Phys. B* **483**, 3 (1997), arXiv:hep-ph/9610231.
- [164] A. Airapetian *et al.* (HERMES), Inclusive Measurements of Inelastic Electron and Positron Scattering from Unpolarized Hydrogen and Deuterium Targets, *JHEP* **05**, 126, arXiv:1103.5704 [hep-ex].
- [165] V. Tvaskis *et al.*, The proton and deuteron F_2 structure function at low Q^2 , *Phys. Rev. C* **81**, 055207 (2010), arXiv:1002.1669 [nucl-ex].
- [166] G. C. Nayak, J.-W. Qiu, and G. F. Sterman, Fragmentation, NRQCD and NNLO factorization analysis in heavy quarkonium production, *Phys. Rev. D* **72**, 114012 (2005), arXiv:hep-ph/0509021.
- [167] J. C. Collins and D. E. Soper, Parton Distribution and Decay Functions, *Nucl. Phys. B* **194**, 445 (1982).
- [168] X. Ji, J. Ma, and F. Yuan, Qcd factorization for semi-inclusive deep-inelastic scattering at low transverse momentum, *Phys. Rev. D* **71**, 034005 (2005), hep-ph/0404183.